

Master Thesis
TVVR 16/5009

ENERGY LOSSES IN HYDRAULIC SYSTEMS OF WATER TREATMENT PLANTS

An application to Vombverket in south
Sweden

IVAN SSENOZI



Division of Water Resources Engineering
Department of Building and Environmental Technology
Lund University

Energy losses in hydraulic systems of water treatment plants

An application to Vombverket in south
Sweden

By:
Ivan Ssenozi

Master Thesis

Division of Water Resources Engineering
Department of Building & Environmental Technology
Lund University
Box 118
221 00 Lund, Sweden

Water Resources Engineering
TVVR-16/5009
ISSN 1101-9824

Lund 2016
www.tvrl.lth.se

Master Thesis
Division of Water Resources Engineering
Department of Building & Environmental Technology
Lund University

English title: Energy losses in hydraulic systems of water treatment plants.
An application to Vombverket in South Sweden.

Author: Ivan Ssenozi

Supervisors: Professor. Magnus Larson.
Tobias Persson and Lars-Anders Fridström
(Sydvatten)

Examiner: Assoc. Professor. Rolf Larsson.

Language: English

Year: 2016

Keywords: Hydraulic system, Energy losses, Local losses, Discharge, Fittings, Pipes, Pipe Flow Expert Model, Loop, Friction losses

Acknowledgements

Firstly, I would like to express my sincere gratitude to my advisors and supervisors, Professor Magnus Larson, Dr. Tobias Persson and Mr. Lars-Anders Fridström for the continuous support, patience, motivation and immense knowledge that have made my master thesis study and research a success. Your guidance helped me all through my research and writing of this thesis. I could not have imagined having better advisors, supervisors and mentors for my thesis work.

Special thanks to the Swedish Institute (SI), for the financial support - Tuition fees and monthly stipends to see me through the two years of my study. You will always be a part of me.

I would like to thank the entire Vombverket team for sharing their pearls of wisdom with me during the course of this thesis work.

My sincere thanks also goes to Associate professor Rolf Larsson and Kate Wicher for their insightful comments and encouragement, but also for the hard questions which incited me to widen my study.

I also thank my fellow classmates for the productive discussions, motivation and for all the fun we had in the last two years.

Last but not the least, I, with great love thank my family: thank you for the everyday support and motivation. You mean the world to me.

I therefore dedicate this report to my lovely son Hayden Troy Kasirye. I love you.

Abstract

Sydvatten AB is a municipally owned company producing and supplying drinking water to about 900,000 inhabitants in southern Sweden through two water treatment plants (WTP), Ringsjöverket and Vombverket.

At Vombverket, the present capacity is somewhat reduced because of pressure losses in the pipe systems of the WTP. Parts of the WTP was built already in the 1950's and it was significantly expanded in the 1990's. In connection with the latter expansion, the transport of water through the WTP was extended before it is pumped to the main pipe system for distribution to the customers. This extension caused increased hydraulic losses in the system, resulting in reduced capacity. The WTP was typically not optimized for the new process design with regard to the hydraulic conditions, but substantial pressure losses were introduced through bends, valves, and other hydraulic components. An alternative to add a pump for overcoming the additional energy losses was to perform a detailed analysis of the flow and establish the location and properties of these losses. This study could form a basis for modifications of the hydraulic system that would reduce the losses and eliminate the need for pumping.

The study begun with a literature review on energy losses in hydraulic systems of WTPs with focus on components present in Vombverket. A thorough investigation of the existing hydraulic system was performed based on available drawings and other additional information, and a comparison made of the system before the WTP was expanded. Measurements of the pressure were carried out at selected points in the hydraulic system in order to quantify the losses occurring in the system.

Based on the knowledge established about the system and the measurement datasets obtained, the hydraulic system was schematized coming up with a simplified conceptual model involving the most important components that were expected to have an effect to the flow. Certain coefficient values were estimated from the collected data on pressure.

Using Pipe Flow Expert, a hydraulic model that had more details and effective description of the complex system was obtained. The model was calibrated, and validated using measured datasets from the plant.

The validated model was then modified to optimize its performance. Financial implications of each modification were done.

There were two significant modifications recommended; (1) To remove specific components from the system, like; weirs, gate valve, and venturi meters. (2) To directly connect the hydraulic system in filter block 1 and 2 to the reservoir, thus shortening the water pathway and reducing energy losses.

Table of contents

| | |
|---|-----|
| Acknowledgements | iii |
| Abstract | v |
| Table of contents | vii |
| INTRODUCTION..... | 1 |
| 1.1 Background | 1 |
| 1.2 Motivation | 1 |
| 1.3 Objectives:..... | 2 |
| 1.4 Procedure..... | 2 |
| LITERATURE REVIEW | 4 |
| 2.1 Theory of fluid flow | 4 |
| 2.1.1 The fundamental principles | 4 |
| 2.2 Governing Equations..... | 5 |
| 2.2.1 Conservation laws | 5 |
| 2.2.2 Energy and hydraulic grade lines | 9 |
| 2.3 Energy losses in hydraulic systems | 9 |
| 2.3.1 Velocity profile in pipes | 10 |
| 2.3.2 Pipe wall friction | 11 |
| 2.3.3 Pipe friction losses | 12 |
| 2.3.4 Empirical expressions | 13 |
| 2.4 Local losses in pipes..... | 14 |
| 2.4.1 Sudden Expansions and contractions | 16 |
| 2.4.2 Gradual expansions and contractions | 17 |
| 2.4.3 Pipe entrance and exit losses | 18 |
| 2.4.4 Flow obstruction components. | 18 |
| 2.4.5 Flow meters | 19 |
| 2.4.6 Bends | 20 |

| | |
|---|----|
| 2.5 Losses in other hydraulic components | 21 |
| 2.5.1 Sand filters..... | 21 |
| MODELLING | 22 |
| 3.1 Modelling pipe system flow | 22 |
| 3.1.1 Pipe Network:..... | 22 |
| 3.1.2 Basic equations..... | 24 |
| 3.2 System Analysis | 24 |
| 3.2.1 System of Q-equations | 24 |
| 3.2.2 System of H-Equations..... | 25 |
| 3.3 Solution methods..... | 26 |
| 3.3.1 Hardy Cross..... | 27 |
| 3.3.2 Newton method | 27 |
| MODELLING SOFTWARE..... | 29 |
| 4.1 Pipe flow expert | 29 |
| 4.1.1 Model structure | 29 |
| 4.2 System schematization | 30 |
| 4.3 Hydraulic components..... | 31 |
| 4.3.1 Fluid source (tanks or reservoirs):..... | 31 |
| 4.3.2 Nodes..... | 32 |
| 4.3.3 Valves and fittings..... | 32 |
| 4.3.4 Entry and exit losses:..... | 34 |
| 4.3.5 Components..... | 34 |
| 4.4 Solution procedure | 35 |
| CASE STUDY SIMULATION | 37 |
| 5.1 Simulation of flow in Vombverket hydraulic system | 37 |
| 5.2 Vombverket hydraulic system..... | 37 |
| 5.2.1 Bends and bespoke fittings..... | 38 |
| 5.2.2 Tees | 38 |

| | |
|---|----|
| 5.2.3 Pipes | 38 |
| 5.2.4 Control valves | 39 |
| 5.2.5 Tanks (reservoirs)..... | 39 |
| 5.2.6 Flow meters | 39 |
| 5.2.7 Rapid sand filters..... | 40 |
| 5.3 Schematization of the system..... | 41 |
| FIELD MEASUREMENTS | 45 |
| 6.1 Measured Datasets..... | 45 |
| 6.1.1 Pressure at selected points in the system..... | 45 |
| 6.1.2 Pressure at the point before the venturi meter..... | 45 |
| RESULTS..... | 55 |
| 7.1 Simulation Results..... | 55 |
| 7.2 Existing system | 55 |
| 7.2.1 Sensitivity Analysis..... | 56 |
| 7.2.2 Calibration | 57 |
| 7.2.3 Validation | 59 |
| MEASURES..... | 62 |
| 8.1 Measures to reduce energy losses | 62 |
| 8.2 Cost implications for all actions made | 65 |
| DISCUSSION, RECOMMENDATIONS AND CONCLUSION | 68 |
| 9.1 Discussion | 68 |
| 9.2 Recommendations | 73 |
| 9.2.1 Category one | 73 |
| 9.2.2 Category two | 74 |
| 9.3 Conclusion..... | 76 |
| REFERENCES..... | 78 |
| APPENDICES..... | 80 |
| Appendix A | 80 |

| | |
|--|----|
| A.1 Analytical derivation of the K-Factor expression | 80 |
| A.1.1 Sudden Expansion and Exit losses into a tank..... | 80 |
| A.1.2 Sudden contraction and entrance losses | 81 |
| Appendix B | 82 |
| B.1 Graphical representations of the experimental determination of the K-factor for pipe fittings..... | 82 |
| Appendix C | 83 |
| C.1 Flow meter characteristics as obtained from manufacturer's catalogues | 83 |
| Appendix D | 83 |
| D.1 System layout for direct connection to the reservoir..... | 83 |

INTRODUCTION

1.1 Background

Sydvatten AB is a municipally owned company producing and supplying drinking water to about 900,000 inhabitants in southern Sweden through two water treatment plants (WTP), Ringsjöverket and Vombverket. The company was founded by five municipalities in Skåne and today serves more than 16 municipalities in the region. It is one of the largest drinking water producers in Sweden and its responsibility is to bring water to the municipal boundary and thereafter the municipality itself is responsible for the delivery to the clients. Sydvatten produces approximately 70 million cubic meters of fresh, healthy and clean drinking water per year which is $2.3\text{m}^3/\text{s}$. Vombverket commenced production in 1948 and produces healthy clean drinking water through a state of the art natural process known as artificial ground water recharge. The plant has two intakes at Vombsjön with a flow rate of approximately $1\text{m}^3/\text{s}$. This water flows through strainers before reaching the 58 infiltration ponds. Here the water is infiltrated to recharge the natural aquifer then pumped up for treatment through 114 wells. Vombverket provides drinking water to Burlöv, Malmö, Staffanstorps, Svedala, Vellinge and some parts of Eslöv and Lund.

1.2 Motivation

At Vombverket the present capacity is rather reduced because of pressure losses in the pipe systems of the WTP. Parts of the WTP were built already in the 1950's and it was significantly expanded in the 1990's. In connection with the latter expansion, the transport of water through the WTP was extended before it is pumped to the main pipe system for distribution to the customers. This extension caused increased hydraulic losses in the system, resulting in reduced capacity.

Therefore, instead of installing a pump to compensate for the additional hydraulic losses introduced, which would require continuous supply of energy and induce extra costs, an option was to carry out a detailed study of the losses in the hydraulic system and how they could be minimized or eliminated through modifications of the system.

To handle and treat water at minimum energy costs is something that Sydsvatten and large parts of the water and sewage sector is constantly working on. In connection with the expansion of WTP or when new equipment is added in the existing system, the transport of water through the system is often prolonged and additional losses occur that reduce the hydraulic capacity - making it necessary to install a new pump. The WTP is typically not optimized for the new process design with regard to the hydraulic conditions, but substantial pressure losses may be introduced through bends, valves, and other hydraulic components. The results of this analysis could form a basis for modifications of the hydraulic system that would reduce the losses and eliminate the need for pumping hence this thesis work.

1.3 Objectives:

The main objective of the study is to investigate the hydraulic system at Vombverket with the purpose of reducing the energy losses that occurred after the expansion of the WTP.

The project involves two sub-objectives:

- Create a model of the hydraulic system between the weir used for mixing (mixing chamber) and the facility for chloramine dosing.
- Investigate different cost-effective measures to modify the hydraulic system that will reduce the energy losses in the WTP.

1.4 Procedure

The study began with a literature review of energy losses in hydraulic systems of WTPs with focus on components present in Vombverket. A thorough investigation of the existing hydraulic system was performed based on available drawings and other additional information, and a comparison made to the system before the WTP was expanded. Pressure measurements were carried out at selected locations in the hydraulic system in order to quantify the losses occurring in the system. The flow was recorded simultaneously.

Based on the knowledge established about the system and the measurement data obtained, a hydraulic model was developed, calibrated, and validated. Certain coefficient values were estimated from the collected data on pressure.

Then, a commercial software for hydraulic modeling called Pipe Flow Expert was procured and applied allowing for a more general and effective description of the system. After proper validation of the model, different modifications to the hydraulic system and their effects on the energy losses were simulated for different operational conditions. An optimum solution with regard to minimizing the energy losses was sought and the economic gains such a solution would generate were quantified.

The work was carried out in close collaboration between Sydvatten and the water resources engineering department at Lund University, with supervisors from both organizations being involved.

LITERATURE REVIEW

2.1 Theory of fluid flow

2.1.1 The fundamental principles

Flow in pipes is classified as being laminar or turbulent. There exists a small region of transition between the two types of flow. It's the non-dimensional Reynolds number that determines the type of flow prevailing in the system. Reynolds number (Re),

$$Re = \frac{VD}{\mu/\rho} \quad (2.1)$$

where the factor μ/ρ is the kinematic viscosity of the fluid, V the mean velocity and D the diameter of the pipe. It is of great importance to specify and know the type of flow in the pipe so as to estimate the amount of energy lost to friction (Cengel and Cimbala, 2006a).

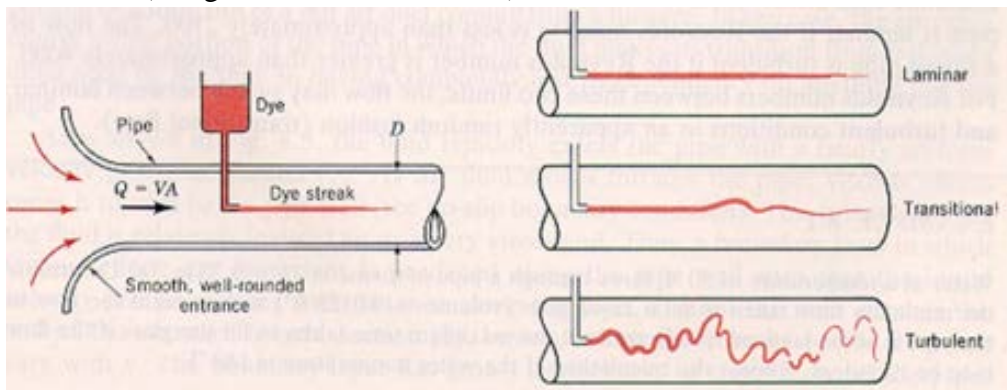


Figure 2-1: Illustration of the laminar, transition and turbulent flows. (Source: Cengel and Cimbala, 2006a).

These types of flow are distinguished by the value of Reynolds number (Re) with the critical value being about 2000.

Laminar flow: $Re < 2000$

Transitional flow: $2000 < Re < 4000$

Turbulent flow: $Re > 4000$

At low values of Re less than 2000, the flow is classified as laminar and that viscosity of the fluid is much more pronounced than inertia and momentum. As the Re increases beyond the critical value, turbulence becomes more important and this leads to an abrupt transition in the flow. Fluid motion resistance tremendously increases but Re beyond the transition region remains majorly influenced by viscosity hence the flow classified as “smooth turbulent” i.e. the boundary layer thickness is greater than the roughness height (Cengel and Cimbala, 2006a). As the Re continues to increase, the influence of turbulence steadily increases as that of viscosity reduces gradually and depending on the pipe surface roughness, at a much higher value of Re , the viscosity of the fluid becomes negligible hence the flow classified as “rough turbulent” i.e. Boundary layer less than roughness height, creating an intermediate zone between the two types of turbulent flow where both viscosity and turbulence are of influence (Ratnayaka, et al, 2009).

2.2 Governing Equations

The fundamental principles of fluid flow are the laws of conservation, which include; conservation of mass, energy and linear momentum. The traditional conservation laws are used to solve fluid dynamic problems and are written in either integral or differential form. The use of finite control volume concept helps to interpret the mathematical formulation of these laws. A finite control volume is a specified volume of space through which a certain specified fluid can flow (Vennard & Street, 1982).

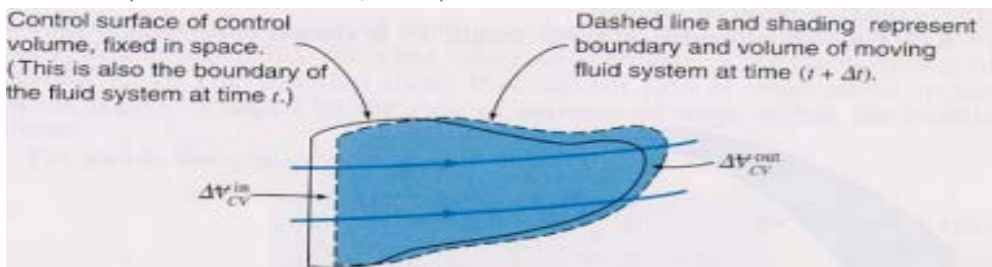


Figure 2-2: Steady state one dimensional finite control volume (Source: Vennard & Street, 1982).

2.2.1 Conservation laws

Firstly, is the conservation of mass also known as the *mass continuity*, the most basic of the principles. This principle requires that mass is neither created nor

destroyed in a specified finite control volume, indicating that the rate of change of the fluid mass must equal to the rate of fluid flow in the control volume. Density, ρ , changes with respect to fluid temperature and is very fundamental in compressible fluid (Larock, et al, 2000). The equation is written as below, considering the pipe section 1 and 2,

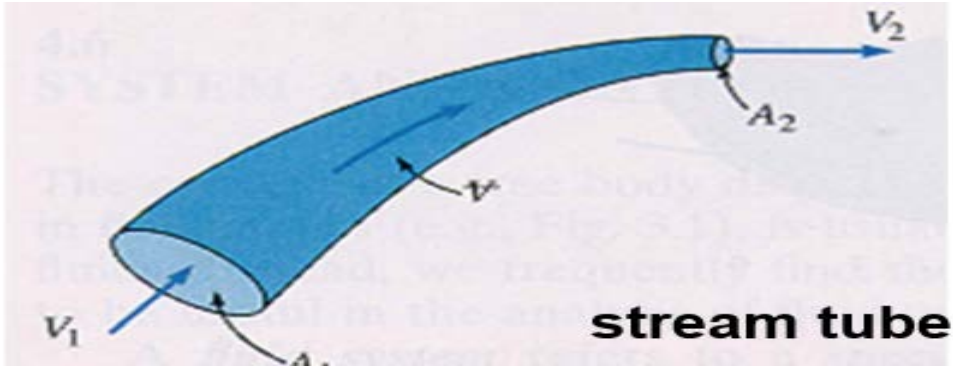


Figure 2-3: Analysis with a pipe section (Source: Cengel and Cimbala, 2006a).

For a one dimensional, compressible fluid at steady state,

$$\rho_1 A_1 V_1 = \rho_2 A_2 V_2 = Q \quad (2.2)$$

Hence, density varies. For an incompressible fluid at steady state,

$$A_1 V_1 = A_2 V_2 = Q \quad (2.3)$$

In which, Q is the volumetric discharge through the pipe section, A, the cross-sectional area of the pipe and, V, the mean velocity of the fluid in the pipe (Cengel and Cimbala, 2006b).

Secondly, is the work-energy principle also known as the conservation of energy or Bernoulli's equation,

$$\frac{V_1^2}{2g} + \frac{P_1}{\gamma} + Z_1 = \frac{V_2^2}{2g} + \frac{P_2}{\gamma} + Z_2 + \sum h_l - h_m \quad (2.4)$$

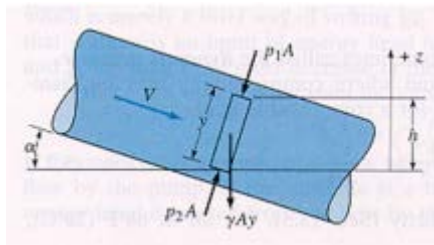


Figure 2-4: illustration of the concept of the equation (Source: Vennard & Street, 1982).

For a unit mass of a fluid, total energy is expressed as a sum of kinetic, potential and pressure energies (work). The principle is written as below for a one dimensional steady flow through the sections as shown in figure 2, including energy input h_m mechanical energy per

unit weight added to the system in case of a pump hence a positive value and a negative value of factor h_t since the turbine extracts energy from the fluid flow (Larock, et al, 2000).

$$\frac{V_1^2}{2g} + \frac{P_1}{\gamma} + Z_1 = \frac{V_2^2}{2g} + \frac{P_2}{\gamma} + Z_2 + \sum h_l - h_m(\text{pump}) + h_t(\text{turbine}) \quad (2.5)$$

In the equation, P , is pressure γ the specific weight (N/m^3) of the fluid equaling to Density (ρ) x Acceleration due to gravity (g), $\sum h_l$ is the summation of both major and minor losses in the system. The function, $\frac{V_1^2}{2g}$ is the velocity head, $\frac{P_1}{\gamma}$ pressure head, $\frac{P_1}{\gamma} + Z_1$ piezometric head, Z_1 the elevation head, and $\frac{V_1^2}{2g} + \frac{P_1}{\gamma} + Z_1$ the total head of section 1 of the pipe (Cengel and Cimbala, 2006b). Energy variation is further illustrated for a fluid element moving from point A to B in a pipe in the figure below;

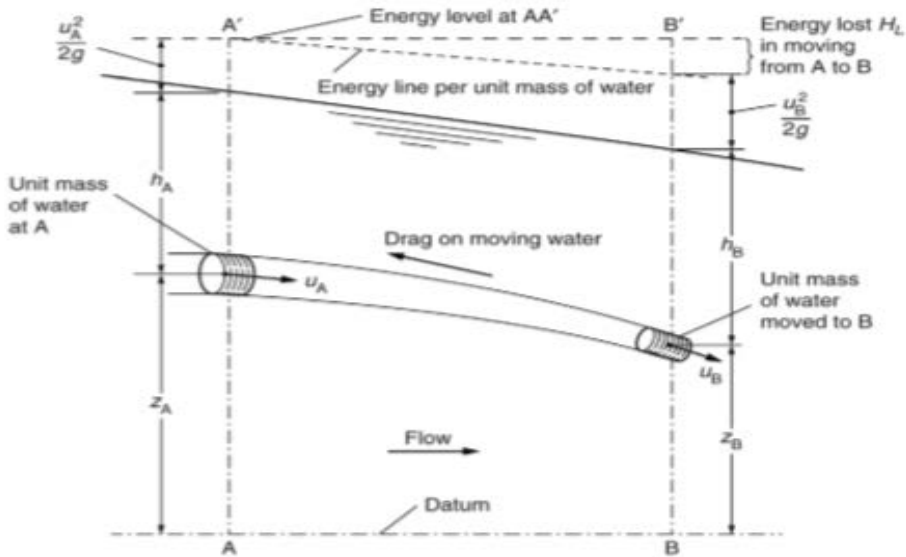


Figure 2-5: Illustration of the variation of energy (Source: Ratnayaka, et al, 2009).

It should be noted that the Bernoulli equation has limitations for instance, it only applies in steady flow problems within a streamline and when there is no energy lost due to turbulence in the flow, hence can be used only during short distance approximations (Cengel and Cimbala, 2006b)

Thirdly and the last of the fundamental principles is the *conservation of linear momentum*, which involves the momentum fluxes and forces. It is widely known as *Newton's second law (with vector relationship)* and illustrated and governed by the impulse –momentum equation stating that, vector quantities of forces (Ratnayaka, et al, 2009):

$$F_{net}^- = F_s^- + F_b^- \quad (2.6)$$

where, F_{net}^- net force, F_s^- surface forces and F_b^- body forces, respectively acting on the contents (i.e. liquid and solid) of the control volume. The net force F_{net}^- is the summation of the rate of accumulation of momentum within a specified control volume (CV) and the net flux of momentum through that CV surface as illustrated in figure 2-6 (Vennard & Street, 1982):

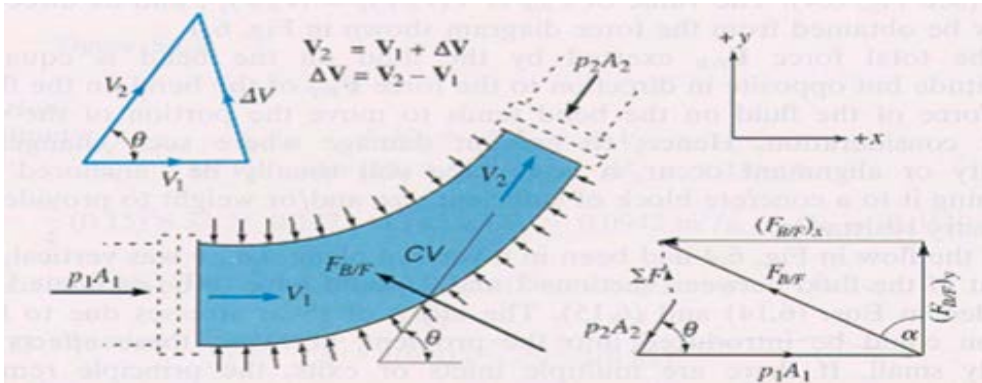


Figure 2-6: Vector relationship for momentum equation analysis (Source: Vennard & Street, 1982).

Therefore, for incompressible, one dimensional flow at steady state, the net force is given by,

$$F_{net}^- = \rho Q(V_2^- - V_1^-) \quad (2.7)$$

For a straight pipe with a constant x-sectional area, $F_{net}^- = 0$, and since we have been dealing with vector quantities (see Eq. 2.7), the equation can always be expressed in any flow dimension. For a 3-dimensional flow, the equation is written in three-dimensions (Ratnayaka, et al, 2009);

$$\begin{aligned} \sum F_x &= \rho Q(V_{2x} - V_{1x}) \\ \sum F_y &= \rho Q(V_{2y} - V_{1y}) \\ \sum F_z &= \rho Q(V_{2z} - V_{1z}) \end{aligned} \quad (2.8a, b, c)$$

2.2.2 Energy and hydraulic grade lines

The energy grade line (EGL), mostly known as the energy line (EL), is as a result of plotting Eq. 2.4 in the direction of flow:

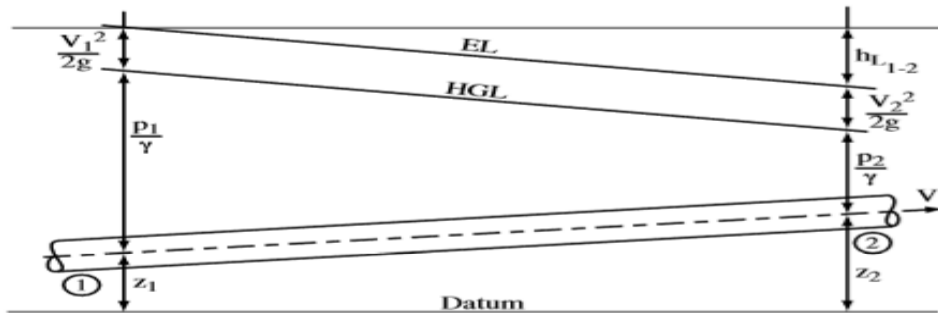


Figure 2-7: Energy line and the Hydraulic Grade line (Source: Larock, et al, 2000).

The hydraulic grade line denoted as HGL, is the plot of the $\frac{P_1}{\gamma} + Z_1$ in the flow direction. It is very easy to locate the HGL provided the location of the EL is known since $\frac{V_1^2}{2g}$ will be the difference (Larock, et al, 2000). Figure 2-7 above clearly exhibits the relationship between HGL and EL for the pipe sectioned 1-2.

2.3 Energy losses in hydraulic systems

From Eq. 2.5, the factor $\sum h_l$ is representative of the sum of the head losses in the specified pipe section and these are of two kinds; losses due to pipe wall resistance to fluid shear, called pipe friction, and the losses due to fluid stream local disruptions in the pipe known as local losses. Pipe friction is always available all through the entire pipe length well as the local losses are due to the bends, flow meters, tee joints, valves and many other pipe fittings of a kind. The local losses are sometimes referred to as minor losses. This is relative because in cases where the pipe friction is minimal i.e. short pipe runs with a lot of bends and other pipe fittings, then the local losses cease to be minor but major and the pipe friction losses may be referred to as minor then. When the minor losses are small, they are at many times during designs neglected.

2.3.1 Velocity profile in pipes

Considering a cylindrical pipe section with, y , as a coordinate with its origin at the pipe wall to the centerline of the pipe with steady fluid flow, and also another coordinate, r , originating from the centerline; therefore, $r = R - y$ for R being the radius of the circular pipe section used as the control volume (Vennard & Street, 1982).

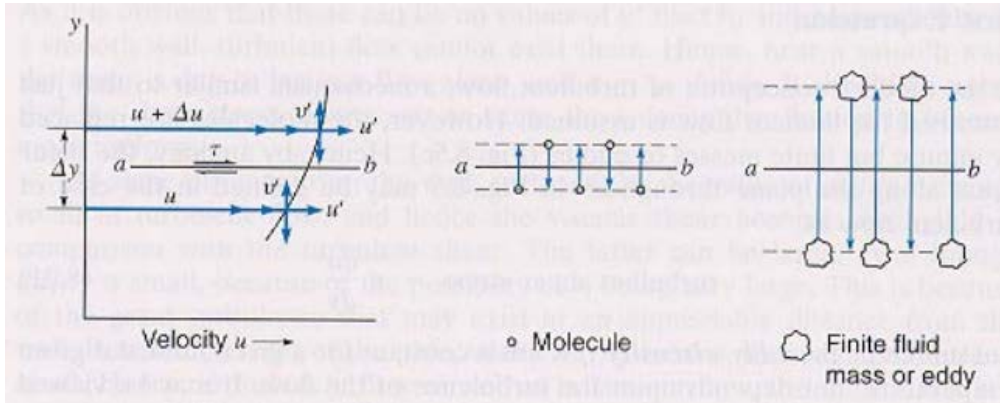


Figure 2-8: Velocity profile in a turbulence model (Source: Vennard & Street, 1982).

Therefore, for laminar flow in a circular pipe section near the pipe wall, the velocity, v , of the fluid can be calculated from:

$$\frac{v}{v_*} = \frac{yv_*}{\nu} \quad (\text{linear velocity profile}) \quad (2.9)$$

and, for turbulent flow, the flow is categorized as either being rough or smooth depending on the wall roughness hence calculating the velocity, v , in the pipe from 2.10 and 2.11 (Vennard & Street, 1982);

Rough turbulent flow i.e. is dependent on the roughness height:

$$\frac{v}{v_*} = 2.5 \ln \left[\frac{y}{e} \right] + 8.5 \quad (2.10)$$

Smooth turbulent flow:

$$\frac{v}{v_*} = 2.5 \ln \left[\frac{v_* y}{\nu} \right] + 5.5 \quad (2.11)$$

where v_* is the shear velocity, e , the roughness height (mm). Taking τ_o to be the wall shear stress

$$v_* = \sqrt{\frac{\tau_o}{\rho}} \quad (2.12)$$

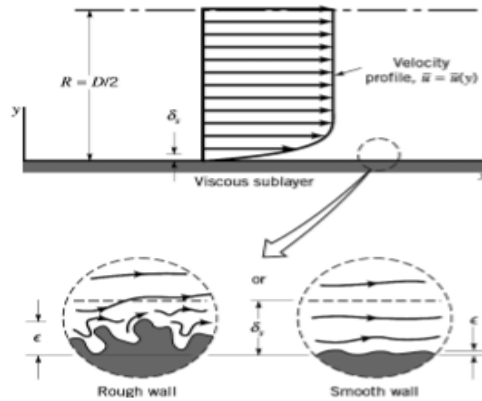


Figure 2-9: Illustration for rough vs. smooth turbulence (Source: Kudela. H, 2001).

2.3.2 Pipe wall friction

The friction head loss h_l over the entire pipe length is considered to be directly proportional to the wall shear stress τ_o is given by;

$$\tau_o = \frac{\gamma R_h h_l}{L} \quad (2.13)$$

where the factor $R_h = \frac{A}{P} = \frac{D}{4}$ is the hydraulic radius of the circular pipe with, A , the area and, P , the wetted perimeter, D , the diameter of the pipe. The shear stress is a function of r and varies linearly from the centerline to the wall of the pipe control volume, but when $r=R$ that's to say when y is equal to zero, then Eq. 2.13 becomes (Larock, et al, 2000):

$$\tau_o = \frac{\gamma R h_l}{2L} \quad (2.14)$$

Therefore, through the use of methods of similitude and dimensional analysis of the function $\tau_o = F(V, D, \rho, \mu, e)$, having noted that the shear stress τ_o depends on fluid viscosity μ , fluid density ρ , mean velocity V , pipe diameter D , and the equivalent roughness height e , the expression below is obtained (Sleigh and Goodwill, 2009):

$$\frac{\tau_o}{\rho v^2} = F \left[\frac{VD\rho}{\mu}, \frac{e}{D} \right] = \frac{f}{8} \quad (2.15)$$

2.3.3 Pipe friction losses

When Eq. 2.14 and 2.15 are combined, the wall shear stress factor is eliminated producing the most fundamental friction head loss equation called the **Darcy-Weisbach formula** sometimes denoted as the D-W Formula.

$$h_l = f \frac{L V^2}{D 2g} \quad (2.16)$$

where, f , is the friction coefficient or factor which is a function of the Reynolds number Eq. 2.1, and the relative roughness, $\frac{e}{D}$ (Sleigh and Goodwill, 2009).

$$f = F \left(Re, \frac{e}{D} \right) \quad (2.17)$$

A single value or range of the equivalent roughness height, e , or, k_s , in mm has been established and the table below presents some of the common values with respect to the materials of the pipe (Vennard & Street, 1982). Note that a roughness value below 0.01mm exhibits an insignificant change in v

Table 2-1: Pipe roughness values $k_s = e$, in mm (Source: Ratnayaka, et al, 2009).

| New clean pipes | k_s , mm |
|---|-------------|
| Steel or ductile iron pipes: | |
| with spun bitumen or enamel finish | 0.025-0.05 |
| with cement mortar lining | 0.03-0.1 |
| Concrete pipes | 0.03-0.3 |
| Plastic pipes | 0.003-0.06 |
| For design with allowance for deterioration: | |
| Raw water mains | 1.5-3.0 |
| Treated water trunk mains | 0.3-1.0 |
| Distribution systems | 0.5-1.5 |
| For new clean service pipes: | |
| Galvanized steel | 0.06-0.30 |
| Copper | 0.002-0.005 |
| MDPE | 0.003-0.006 |
| PVC-U | 0.003-0.06 |

The friction factor, f , is in detail displayed in the Moody diagram in figure 2-10. It is in this figure that all the zones characterizing the pipe flow types are shown. The f -value can be obtained for the figure below once the Reynolds number or the relative roughness is known (Sleigh and Goodwill, 2009).

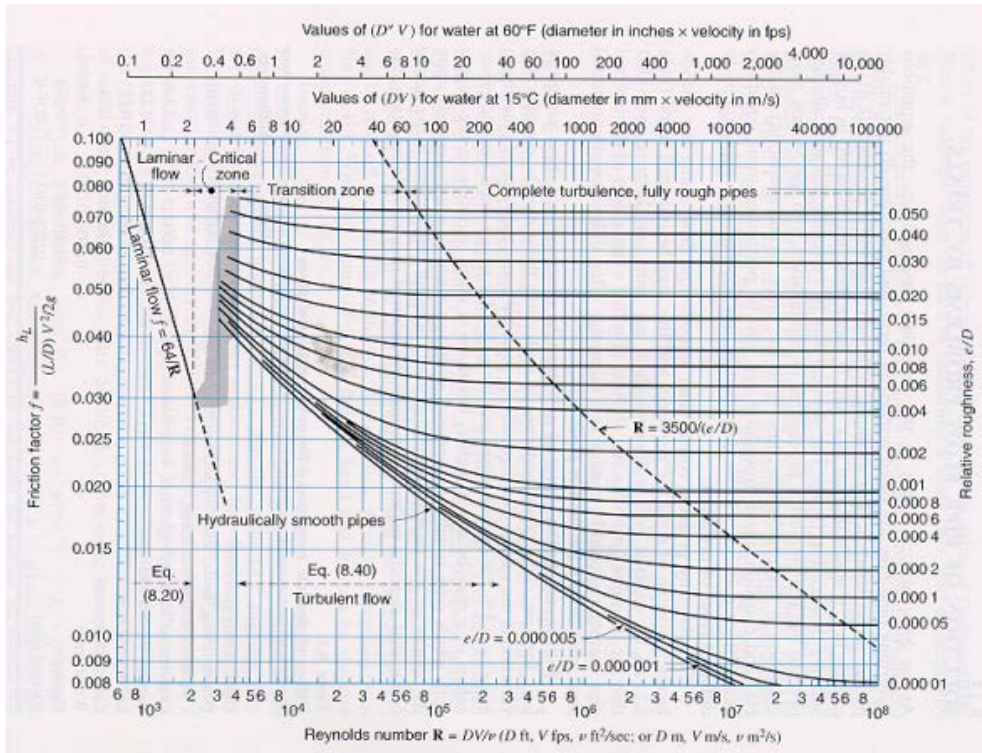


Figure 2-10: The Moody diagram (Source: Vennard & Street, 1982).

2.3.4 Empirical expressions

In the Moody diagram, fig. 2-10 above, it's observed that the zone where the Reynolds number, $Re = 2100$, one line is appearing. This line represents laminar flow, and the friction factor, f , can be calculated from,

$$f = \frac{64}{Re} \quad (2-18)$$

Therefore, this means that in laminar flow, all pipes are considered to be hydraulically smooth (Vennard & Street, 1982).

The dashed line on top in the upper right part of fig. 2-10, is the zone representative of the completely turbulent flow in a fully rough pipe. In this zone the friction factor, f , is a function of only the relative roughness (e/D) which is common in large discharges for relatedly rough pipes. So once the, e/D , value is known, the f -value can be read off from the moody diagram (Sleigh and Goodwill, 2009).

For rough flows, the value of, f , can also be obtained from the empirical expression,

$$\frac{1}{\sqrt{f}} = 2.0 \log \left(\frac{D}{e} \right) + 1.14 \quad (2-19)$$

The lower full line in diagram 2-10 is a representation of the smooth pipes with relatively significant turbulence. This is dependent of Reynolds number only. Once the Reynolds number is known, the value for the friction factor can be read off from the left y-axis of the Moody diagram.

The value of the friction factor can also be obtained from the empirical expression below with iterations involved (Larock et al, 2000);

$$\frac{1}{\sqrt{f}} = 2.0 \log(Re\sqrt{f}) - 0.8 \quad (2-20)$$

In between the smooth line and the fully rough line is the turbulent transition zone in which the friction factor is a function of both relative roughness and Reynolds number as shown in Eq. (2-17). The **Colebrook-White equation** is applied to calculate the friction factor, f , especially by hydraulic computer model to numerically replicate this zone's data as in the figure (2-10) (Larock, et al, 2000). Colebrook-White equation is,

$$\frac{1}{\sqrt{f}} = 1.14 - 2 \log \left(\frac{e}{D} + \frac{9.35}{Re\sqrt{f}} \right) \quad (2-21)$$

Pipe friction calculations are based on the unpredictable changes in the, e , and, f , values due to many factors such as; dirt accumulation in the pipes, corrosion and the pipe age among others. These tend to not only affect the pipe roughness but also the effective diameter of the pipe leading to enormously high f -values especially for older pipes (Kudela. H, 2001), see table 2-1.

2.4 Local losses in pipes

These are sometimes referred to as minor losses, they are losses that occur at a specific point in a pipe and are calculated using the general expression

$$h_l = K_l \frac{V^2}{2g} \quad (2-22)$$

where, K_l is a coefficient that depends on the nature of the loss in the pipeline (Kudela. H, 2001). The losses are as a result of additional components to the straight pipe network. They are as a result of local disruption of fluid flow in

the pipe by hydraulic components apart from the pipe itself (Vennard & Street, 1982). These include but not limited to;

- Pipe entrance and exit from a tank
- Sudden expansions and contractions
- Gradual expansions and contractions
- Flow obstruction components such as, valves; open or partially closed
- Pipe fittings like, bends, 90⁰- 45⁰ elbows and tees among others
- Flow meters, Venturi meters
- Filtration systems, sand filters (rapid or slow)

Most commercial pipe fittings manufacturers provide the K_f value that they obtain through experiments. The head losses are determined using Eq. 2-22 above.

Consider an abrupt obstruction in a pipe section fig. 2-11, energy is dissipated as a result of flow conditions typical of minor losses. As velocity of water particles in the pipe increases, the pressure decreases and the reverse is true. The value of K_f increases as the pipe wall roughness increases with decreasing Reynold's number. These variations are of insignificant influence in turbulent flow (Vennard & Street, 1982). In Fig 2-11, Vennard and Street further depict scenarios where energy is dissipated creating minor losses in pipe flow due to the eddies formed as the liquid decelerates just after the constriction. Sections 1 and 2 indicates constriction, 2 and 3 energy extraction due to eddy creation, 3 and 4 established turbulent flow due to decomposition of the eddies.

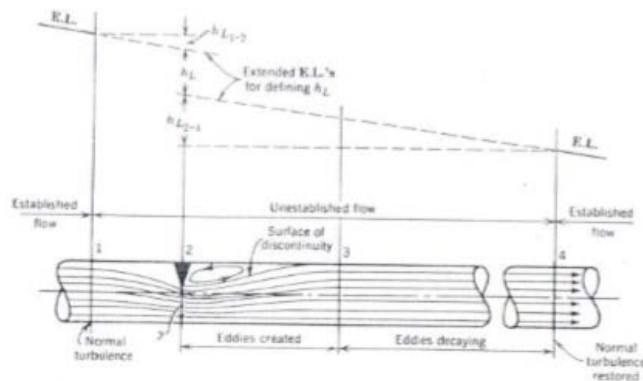


Figure 2-11: Analysis of minor losses in pipelines (Source: Vennard & Street, 1982).

2.4.1 Sudden Expansions and contractions

Figure 2-12, is representative of a pipe section with a sudden expansion which leads to a rapid deceleration of water particles, separation or creation of vigorous eddies which can propagate through large pipes for a distance equivalent to 50 diameters and more before established turbulent flow is attained again (Vennard & Street, 1982).

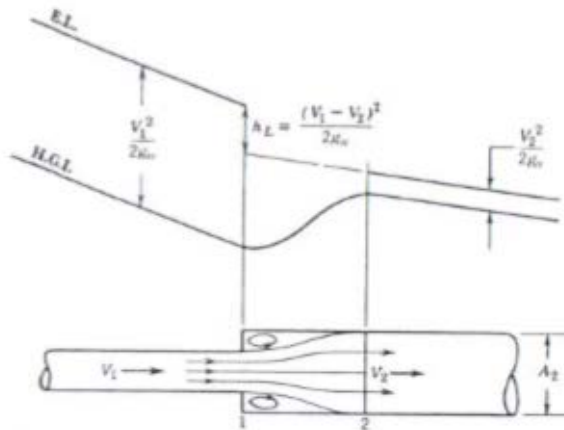


Figure 2-12: Illustration of an abrupt expansion (Source: Vennard & Street, 1982).

Velocity v_1 , is the velocity upstream of the expansion and is the one considered during calculation for the head loss using equation 2-22.

For a sudden contraction in figure 2-14 below, the velocity v_2 instead, is used to calculate for the head loss using equation 2-22. The vena contracta represents the maximum velocity section.

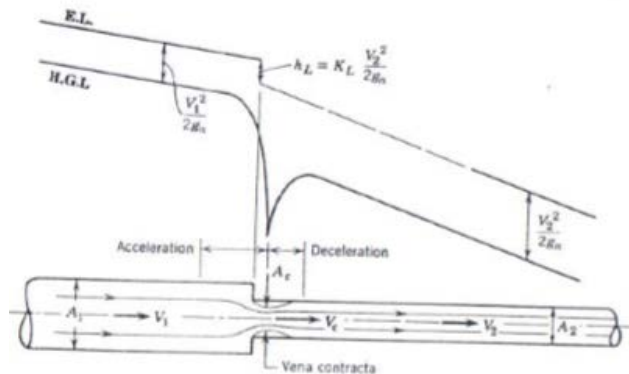


Figure 2-13: Sudden contraction (Source: Vennard & Street, 1982).

With application of the continuity, Bernoulli and the momentum principles simultaneously will lead to the expression (2-23), where v_1 and v_2 are the velocities shown in the figures 2-12 and 2-13 respectively.

$$h_l = K_l \frac{(v_1 - v_2)^2}{2g} \quad (2-23)$$

The value of K_l can also be obtained from figure 11-1 for sudden enlargement and figure 11-2 for sudden contraction (fig. 11-1 and 11-2 are in the appendix).

2.4.2 Gradual expansions and contractions

The shape of the gradual enlargement will determine the magnitude of the loss incurred, as from fig. 2-14, K_l is dependent of the angle of enlargement and some what the length of enlargement. At very low angles, the energy loss coefficient K_l will depend wholly on the pipe wall friction and as the angle becomes bigger and more abrupt, the coefficient depends on turbulence which is as a result of separation or eddies created. Fig. 2-14 shows an optimum cone angle of approximately 7 degrees for minimum wall friction and eddy turbulence effect. Maximum value of K_l at cone angle 70 degree (Vennard & Street, 1982).

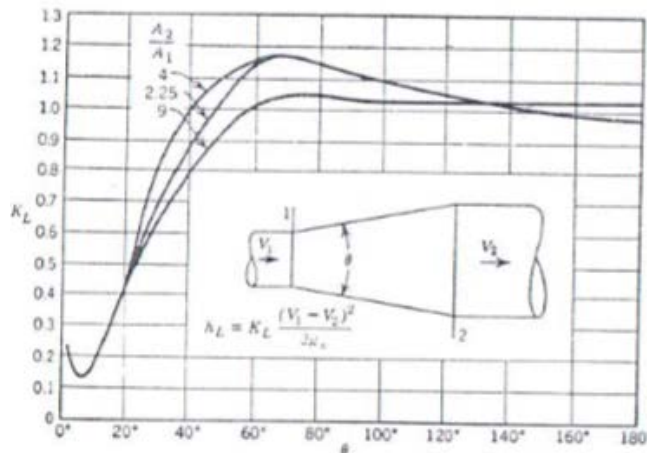


Figure 2-14: Loss coefficient K_l for gradual enlargements (Source: Vennard & Street, 1982).

With a small angle of enlargement (diffuser), there is recovery of energy in the direction of fluid flow because there is less separation, deceleration of water particles and the HGL is seen to rise and the EL decreases. See figure 2-14.

The head losses due to gradual contractions in a short well- stream lined section can be so small that it can be neglected in most design tasks. The K_L Value for such a scenario is less than 0.04 for short well-streamlined contractions and greater than 0.04 for longer contractions due to prolonged surface friction (Vennard & Street, 1982).

2.4.3 Pipe entrance and exit losses

Entrance losses are as a result of a square-edged, re-entrant, bell-mouthed or round pipe entrance as shown in the figure 2-16a and b below

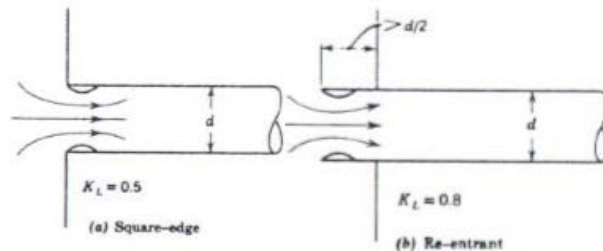


Figure 2-15: square edged and re-entrant pipe entrances (Source: Vennard & Street, 1982).

The head loss is calculated from Eq. 2-22, where the K_L value is approximately 0.5 during high turbulence for the square-edged entrance and approximately 0.8 for the re-entrant, Fig. 2-16b, when the pipe wall is significantly thin with one diameter reentrancy into the reservoir from the wall. For a slightly rounded and bell mouthed entrances, the K_L value is highly reduced as shown in table 2-2.

2.4.4 Flow obstruction components.

These include valves and many other components. Valves are classified based on these function, this can be as isolating, regulating and control valves in addition to other functions such as air/vacuum release, checking/ back flow prevention, pressure relief and pressure sustaining valves among others.

Isolating valves are used while fully open or closed but never partially open unless designed for such purpose and in this case it functions more like a regulating valve (Crane co, 1988).

Regulating valves are somewhat flexible in use since they can be left partially open in throttled conditions and therefore, the head lost is a function of the flow through the valve depending on the degree of opening. They are used in

balancing pressures downstream and at no flow the downstream pressure equates the upstream (Ratnayaka, et al, 2009).

Control valves are used in conditions that require frequent adjustments most especially in automated systems. These valves don't guarantee drop-tight hence can't protect the downstream system from extreme static pressures (Crane co, 1988).

Which valve to use, always depends on the size of the pipes, the pressures being dealt with, price, and the type of flow for-example, butterfly valves are much cheaper than gate valves, easy to operate especially in systems with unbalanced pressure like gravity flow schemes. Table 2-2 below, gives the experimentally measured values of the loss coefficients of different types of valves which can then be used in Eq. 2-22, to calculate the head losses through each valve. These coefficient values are also provided by the manufacturers of the valves.

2.4.5 Flow meters

Flow meters are classified as either volumetric or inferential. Inferential flow meters are the ones that use variables like pressure differences over a device like an orifice to determine the velocity of water hence obtaining the flow. These meters include the Venturi meters and many others.

Volumetric flowmeters: there are many types of these meters for-example, electromagnetic, ultrasonic, coriolis, vortex, turbine or propeller flow meters among others. A table with other types of meters and their characteristics is attached in the appendix (see table 11-1). An in-depth description is presented below for one of each flowmeter types, volumetric and inferential respectively (Ratnayaka, et al, 2009).

Electromagnetic flowmeters offer no obstruction to the flow path and is the most versatile flowmeter today. They are based on Faraday's law of electromagnetic induction in which the velocity, V , of the conductor is considered to be equal to the velocity of the liquid flowing through the tube. The length of the conductor, D , is equal to the distance between the electrodes, the magnetic flux strength, B , and, E , as the voltage between the electrodes (Ratnayaka, et al, 2009). The expression for solving for, V , is given below;

$$E = KBDV \quad (2-24)$$

where, K , is the proportionality constant, therefore Q can be obtained once V is known. These flowmeters are widely used in the water distribution sector because of their **zero head loss** characteristic, reliability and accuracy in flow measurement (Ratnayaka, et al, 2009).

Venturi meters: these are inferential flowmeters. The liquid accelerates as it flows through the constricting cone with an angle in the ranges of 15-21 degrees for efficiency before it gets to the throat of a specific size. Using Eq. 2-4, Bernoulli Equation between the upstream end and the throat of the venturi, the pressure drop across the device is determined. The diffuser portion of the venturi is for pressure recovery and this is possible only when the angle of enlargement is made as small as possible over a longer distance. An angle between 5-7 degrees is appropriate so that the kinetic energy is converted back to pressure energy. If the angle of the diffuser is made bigger than the optimum angle range then there will be separation and eddy creation which will prohibit the pressure recovery process leading to very high pressure drops across the device (Ratnayaka, et al, 2009).

2.4.6 Bends

Commercial bends, that's to say, 90 and 45 degree elbows, long and, standard, have their loss coefficient value determined experimentally by the manufacturers. The losses in these fittings is as a result of change of flow direction. As fluids flow through bends there is a condition of "secondary flow" created. This condition is of rotation motion nature at right angles with the pipe axis created by a combination of pipe-wall friction resistance and the centrifugal force. Energy loss in the bend comprises of: loss caused by curvature (hence change in flow direction), downstream tangent loss and length induced loss (Crane co, 1988).

Caution must be taken when choosing the bend shape to optimize the system efficiency during design basing on the, R/D ration, see table 2-2.

Table 2-2: Loss coefficients for pipe fittings (Source: Vennard & Street, 1982).

| Fitting Type | | K | Fitting Type | | Fitting | | K _L |
|----------------------------------|--|------|--------------------------------|--|---------|-------------------------------------|----------------|
| Pipe Entry Losses | | | Global Enlargements | | | Globe valve, fully open | 10.0 |
| Round inlet | | 0.50 | Ratio d/D = 1/2 typical | | 0.50 | | |
| Flare inlet | | 0.05 | Ratio d/D = 1/2 typical | | 0.50 | Angle valve, fully open | 5.0 |
| Flange flanged inlet | | 0.25 | Ratio d/D = 1/2 typical | | 0.50 | Butterfly valve, fully open | 0.4 |
| Refractured inlet | | 0.05 | Ratio d/D = 1/2 typical | | 0.50 | Gate valve, fully open | 0.2 |
| Pipe Intermediate Losses | | | Valves | | | Gate valve, 3/4 open | 1.0 |
| Elbow 90° <math>r/D < 0.5</math> | | 0.25 | Ball Valve (fully open) | | 0.20 | Gate valve, 1/2 open | 5.6 |
| Long Radius Elbow (R/D = 2) | | 0.20 | Ball Valve | | 2.00 | Gate valve, 1/4 open | 17.0 |
| 90° | | 0.20 | Plug Valve | | 10.00 | Check valve, swing type, fully open | 2.3 |
| 45° | | 0.25 | Gate Valve | | 10.00 | Check valve, lift type, fully open | 12.0 |
| Tee | | 0.25 | Butterfly Valve (fully open) | | 0.20 | Check valve, ball type, fully open | 70.0 |
| (a) Flow in line | | 0.25 | Angle Valve | | 1.00 | Foot valve, fully open | 15.0 |
| (b) Line to branch flow | | 1.00 | Angle Valve | | 1.00 | Elbow, 45° | 0.4 |
| Radius Enlargements | | | Fast Valve with orifice | | | Long radius elbow, 90° | 0.6 |
| Ratio | | 0.50 | Ratio | | 10.00 | Medium radius elbow, 90° | 0.8 |
| 0.5 | | 0.50 | Ratio | | 10.00 | Short radius (standard) elbow, 90° | 0.9 |
| 0.7 | | 0.70 | Ratio | | 10.00 | Close return bend, 180° | 2.2 |
| 0.9 | | 0.90 | Ratio | | 10.00 | Pipe entrance, rounded, r/D < 0.16 | 0.1 |
| 1.0 | | 1.00 | Ratio | | 10.00 | Pipe entrance, square-edged | 0.5 |
| Radius Contractions | | | Air Valves | | | Pipe entrance, re-entrant | 0.8 |
| Ratio | | 0.50 | Ratio | | 0.10 | | |
| 0.5 | | 0.50 | Ratio | | 0.10 | | |
| 0.7 | | 0.70 | Ratio | | 0.10 | | |
| 0.9 | | 0.90 | Ratio | | 0.10 | | |
| 1.0 | | 1.00 | Ratio | | 0.10 | | |
| Flow-Field Losses | | | Half Valve | | | | |
| Square Outlet | | 1.00 | Ratio | | 0.10 | | |
| Round Outlet | | 0.50 | Ratio | | 0.10 | | |
| Round Outlet | | 0.50 | Ratio | | 0.10 | | |
| Round Outlet | | 0.50 | Ratio | | 0.10 | | |
| Round Outlet | | 0.50 | Ratio | | 0.10 | | |

2.5 Losses in other hydraulic components

In complex water distribution systems, there are several other hydraulic components that provide additional energy losses to the system. Some of these components' losses are so insignificant that they are neglected for example, filtration systems like sand filters, hydraulic structures like weirs and many others.

2.5.1 Sand filters

Filtration is a process used widely in the water industry for separation, removing fine organic and inorganic particles from water. Sand filters are filtration systems with the filtration medium being granular material such as sand, activated carbon, anthracite and many others. The types that are commonly used in drinking water treatment plants is the rapid sand filtration and slow sand filtration. When clean, the water flows with ease hence limited head losses but as they stay in operation for a given time and depending on the quality of the raw water, the fine material in the water builds up on to the filter material hence increased resistance to flow. This resistance increases to a certain limit and triggers a backwash so as to clean up the filter before it's reused all over again. This is a continuous process in a treatment plant.

MODELLING

3.1 Modelling pipe system flow

Modeling pipe systems is done with a basis on the basic principles, that is; the conservation of mass, *equation 2.3* and conservation of energy, *equation 2.4* as discussed in chapter two of this report.

With an assumption that, all the physical system features such as pipe diameters, length, roughness, and individual vital component locations are known and the only parameters to find are the discharge and pressure at all nodes in the network. During pipe network analysis, it's always vital to start by identifying the most important features of the system and ensure that they are detailed and well defined. Schematization should be the first step during large systems analysis because it will help to specify the most important aspects and components to consider during the analysis. During schematization; (1) not all connections are represented as distinct nodes and junctions but rather some can be summed-up or combined as one node. (2) only the major and most vital distribution system is considered and presented. (3) only major components with a significant impact on the system could be considered (Larock, et al, 2000).

3.1.1 Pipe Network:

Pipe networks are classified into two types, that's to say, *branched and looped pipe networks*. The number of equations will be directly proportional to basic relationships between the number of pipes, nodes and loops that occur in both types of networks. These relationships are denoted as, NP, for number of pipes, NJ, as the number of junctions and, NL, the number of loops in the network around which individual equations are written. A node or junction is defined as a single point at which two or more pipes meet. A node may not specifically be a point of any energy loss but rather a joint for pipes. In branched networks, NL, is zero since there are no complete loops and the number of pipes is always one less than the number of nodes or junctions in the system. Reservoirs are not considered as nodes so when they appear in a system then, $NP = NJ$.

Figures 3-1 and 3-2 illustrate small branched and looped pipe networks respectively (Larock, et al, 2000).

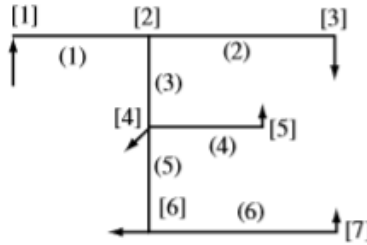


Figure 3-1: A branched pipe network with 6 pipes, 7 nodes (Source: Larock, Jeppson, & Watters, 2000).

The number of pipes in a branched network is calculated by,

$$NP = NJ - 1 \quad (3-1)$$

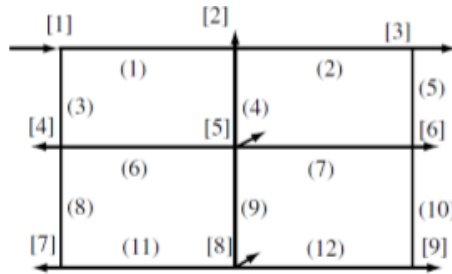


Figure 3-2: A looped pipe network with 12 pipes, 9 nodes and 4 loops (Source: Larock, et al, 2000).

For a looped network like the one in figure 3-2, the number of loops is calculated from,

$$NL = NP - NJ \quad (3-2)$$

Larock, Jeppson, & Watters, (2000) noted that, for networks with two or more supply sources, Eqn. 3-2 applies, and when the system is composed of less than two supply systems, the equation becomes 3-3 below having considered the single source as a node and presented as a negative demand;

$$NL = NP - (NJ - 1) = NP - NJ + 1 \quad (3-3)$$

Therefore, the basic relations below for the flow in pipe networks are valid:

1. Flow into and out of a specific node must be equal for continuity
2. The pipe friction law must be valid in each pipe in the system
3. The algebraic sum of all the head losses must be equal to zero for any closed loop in the network.

3.1.2 Basic equations

There are two basic principles governing the pipe network analysis, and these are; 1) the *conservation of mass*, Eqn. 2.3, also known as the *continuity equation*, 2) the *work-energy principle* Eqn. 2.4, or *Bernoulli's equation*. The equations developed from the conservation of mass principle are referred to as the *junction continuity equations*. These depicts the fact that, the sum of all the flows in and out of a junction must equal to the demand (Boulos & Altman, 1991).

$$\sum_i Q_i = QJ_j \quad (3-4)$$

And *energy loop equations* are equations derived from the *Bernoulli equation*. Meaning that the algebraic sum of all energy losses around any closed loop is equal to zero (Larock, et al 2000).

$$\sum_i h_{Li} = 0 \quad (3-5)$$

$$\sum_i (K_i Q_i^n) = \sum_i (K_i |Q_i| Q_i^{n-1}) = 0 \text{ (real) or } = \Delta WS \text{ (pseudo)} \quad (3-6)$$

A pseudo loop is an energy loop starting at one supply source and end at the other

3.2 System Analysis

For steady flow in pipe networks, there are three different equation systems that can be developed during pipe-network problems analysis. These equation systems are based on the principle variables that are unknown in the solution method as categorized below (Larock, et al, 2000).

1. **Q-equations**; are equations used when the discharges in the pipe network are the principle unknown variables.
2. **H-equations**; are equations for pipe networks in which the HGL-elevations, known as the heads, H, at the nodes, are the major unknown variables
3. **ΔQ -equations**; for pipe networks in which the corrective discharges, ΔQ , are the principle unknown variables

3.2.1 System of Q-equations

As noted before, the pipe network problems analysis is based on two principles, continuity and work-energy equations, therefore, for continuity to prevail, the volumetric discharge in and out of a specific node must be equal, see Eqn. 3-

4. In which, Q_j , denoted the demand at node, j, and, Q_i the discharge in one of the pipes at that node. The continuity equations at the junctions represent the first set of the Q-equations (Larock, et al, 2000).

The second set of Q-equations is derived from the work-energy principle, which are a summation of energy losses along both real and pseudo loops. The Q-equations for real and pseudo loops respectively, are presented below (Larock, et al, 2000);

$$\sum(h_f) = 0 \quad (3-7a)$$

$$\sum(h_{fi}) = \Delta WS \quad (3-8a)$$

Expressing the energy losses in terms of exponential formula, Eqn. (3-7a) and (3-8a) will take the form of Eqn. 3-6 above.

3.2.2 System of H-Equations

When the hydraulic grade line in the pipe network is the limiting factor or the principle unknown variable, then, one H-equation is written at each node for less than two supply sources.

The exponential equation of discharge below is solved in order to derive the H-equations,

$$Q_{ij} = \left(\frac{h_{fij}}{K_{ij}} \right)^{1/n_{ij}} = \left[\frac{(H_i - H_j)}{K_{ij}} \right]^{1/n_{ij}} \quad (3-9a)$$

The frictional energy loss h_{fij} is considered to be equal to the HGL values' difference $(H_i - H_j)$ between the upstream node, i, and downstream node, j. Equation 3-9a can also be written in terms of pipe number, k, where $ij = k$ giving equation 3-9b (Larock, et al, 2000).

During the analysis, Eqn. 3-9a and the continuity equations will help solve the pipe-network problem shown in figure 3-3 below.

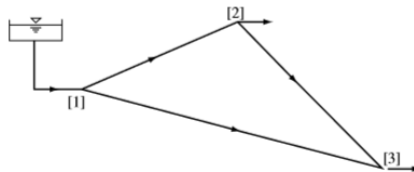


Figure 3-3: A simple pipe network with 3 pipes and 3 nodes.

The two junction continuity equations will be written as

$$Q_{12} + Q_{13} = QJ_1 = QJ_2 + QJ_3 \quad (3-10a)$$

And

$$Q_{21} + Q_{23} = -QJ_2 \text{ or } (-Q_{12} + Q_{23} = -QJ_2) \quad (3-10b)$$

Direction of flow is put in consideration hence the signs. Therefore, substituting Eqn. 3-9 into these equations 3-10a and, b, will lead to the system of H-equations (Larock, et al, 2000).

3.2.3 System of ΔQ -equations

Larock, Jeppson, & Watters, (2000), states that, the number of *H-equations* is about twice the number of ΔQ -equations for any pipe network. In this kind of problem, the corrective discharges are considered to be the principle unknown variables. The ΔQ 's are derived from the work-energy equations for the loops in the pipe network, so the number of loops for this network must be determined.

$$Q_i = Q_{Oi} + \sum \Delta Q_k \quad (3-11)$$

This means that the discharge Q_i in each pipe of the network is equal to the sum of the initial discharge, Q_{Oi} , and the summation of all the unknown corrective discharges through pipe i. equation 3-11 is then substituted in equation 3-6 respectively to obtain the ΔQ -equations. In all this work the head loss is expressed in form of exponential formula (Larock, et al, 2000).

$$h_f = KQ^n \quad (3-12)$$

This doesn't matter whether it's the D-W equation, Hazen-Williams equation, or Manning's equation used. It's only the, K, and, n, values that will change. In this report we are using the D-W equation, Eqn. 2-16.

3.3 Solution methods

In section 3.1.3, I reconnoitered how to write the systems of equations in large pipe networks and noted that most of these equations are nonlinear. Therefore, the most appropriate and better method of solving these equations is needed to be employed. There are many methods in existence Hardy Cross, Newton-Raphson, linear theory and electric-network analyzer methods among others but below is the Hardy Cross and the Newton methods discussed.

3.3.1 Hardy Cross

As it was noted in the initial statements in section 3.1, that it's assumed that all the physical system features like pipe sizes among others and the network schematization and elevations are known and in place. The unknown are pressure and discharges at each node. The solution to this problem can be obtained through an iterative process and in this case the famous Hardy Cross method. The trick behind the method is to assume reasonable initial values of flowrates fulfilling continuity at each node in the network and these are systematically adjusted until when the head losses equations (D-W equation) are satisfied to a reasonable degree, see equation 3-12. The summation of all losses in each loop must equal to zero (Vennard & Street, 1982).

Flowrates are corrected basing on flow correction expression 3-13, below;

$$Q_i = Q_{oi} \pm \Delta_L \quad (3-13)$$

where, Δ_L , is the correction factor and the other denoted symbols are as in Eqn. 3-11. When the precaution that, 'summation of all losses in each loop = zero' see Equation 3-14, then solution found otherwise cycle through again (Vennard & Street, 1982).

$$\sum_i h_{Li} = \sum_i (\pm)_i K_i Q_i^n = \sum_i (\pm)_i K_i (Q_{oi} \pm \Delta_L)^n \quad (3-14a)$$

$$\approx \sum_i (\pm)_i K_i (Q_{oi} \pm n Q_i^{n-1} \Delta_L) = 0 \quad (3-14b)$$

Vennard & Street, (1982) finally gives the expression for the correction factor, Δ_L , as Eqn. 3-15 below

$$\Delta_L = - \frac{\sum_i (\pm)_i K_i Q_i^n}{\sum_i |K_i n Q_i^{n-1}|} \quad (3-15)$$

3.3.2 Newton method

After the introduction of computers in the 1960s, the Hardy Cross method that had become the basis for most of the computer software then, had issues with convergence especially for larger systems that consisted of several components such as pumps, pressure relief valves (PRV), and Back pressure valves (BPV) plus thousands of pipes in the network which made it hard to solve these problems. This led to the Newton method. Over the following years, the Newton method has proved to be much more effective and appropriate in solving nonlinear equation as it's used to code computer software. All the

system of equations discussed in section 3.2 above are easily solved by the Newton method (Larock, et al, 2000).

The Newton iterative formula, is written as;

$$\{x\}^{m+1} = \{x\}^m - [D]^{-1}\{F\}^m \quad (3-16)$$

where, x , denotes an entire column vector $\{x\}$ of unknowns, $\{F\}$ the entire column vector of equations and the inverse of the matrix $[D]$ known as a Jacobian (Larock, et al, 2000).

MODELLING SOFTWARE

4.1 Pipe flow expert

Pipe flow expert is a commercial software application used for pipe systems' hydraulic modelling by professional engineers in more than 75 countries in the world to calculate flow rates, energy losses and pump sizing and requirements. The pipe designs can be drawn on both 2D and 3D isometric grids.

4.1.1 Model structure

The software helps to ease drawing and analysis of pipeline systems performance as fluids flow through. The software calculates hydraulic system requirements and performance analysis at various operation conditions. The input and display data in the model can be expressed in metric or imperial units and also different units can be assigned to specific parameters/items individually depending on the modeler's preference.

At the end of the model calculations, the following parameters are included in the results report.

- Reynolds number
- Friction factor
- Flow rates through each individual pipe
- Fluid velocities per pipe
- Friction energy losses (pressure drop)
- Fitting pressure losses
- Component pressure losses
- Pressure at each individual node
- Value of the hydraulic grade line
- Pump operating points
- Available net positive suction head (NPSHA) at pump inlet

The pipe hydraulic systems can be as simple as a single pipe system conveying water from one point to another, or large complex fluid/water distribution networks with hundreds of thousands of pipes. The network may include pipelines of varying sizes, different materials, elevations changes from point-

to-point, reservoirs, looped-systems, valves, pumps, flow control devices (BPVs & PRVs), flow meters, heat exchangers, filtration devices and many other components that affect flow in hydraulic systems.

The modeler can draw and make use of horizontal, vertical or slanting lines representative of pipes to join different nodes in the system and will have to input the following data and specify various boundary conditions.

- The pipe internal, nominal and outside diameters,
- Individual pipe thickness, length and material
- Any external inflow and out flow at each node (if applicable)
- The individual node elevations
- If reservoirs/tanks are present then, the liquid level, surface pressure and elevation must be included.
- The pump performance data

There are data input display tables on the left-hand side of the drawing pane/grid. These data boxes are specifically for the node on top and pipe at the bottom and the modeler can do data adjustments in these tables at any stage of the modelling process provided not in the results mode.

4.2 System schematization

This process is also called “skeletonization” or simplification of network model components and involves the exercise of drawing the system model layout, selection of which parts or components of the hydraulic network are of great impact and pose a significant effect on fluid flow behavior, to be included in the model. The degree of schematization will depend highly on the level of accuracy required and the model intent. The skeletonization process takes time and in most cases will depend on the experience of the modeler for choice. It will include

- Combining nodes of the same characteristics into one instead of having many separated ones.
- Use of equivalent pipe length instead of some fittings/ components.
- Deletion of always closed pipes.
- Elimination of small capacity tanks and very short pipe runs

- Removal of unnecessary pipe sections brought about by irrelevant valves and fire hydrants.

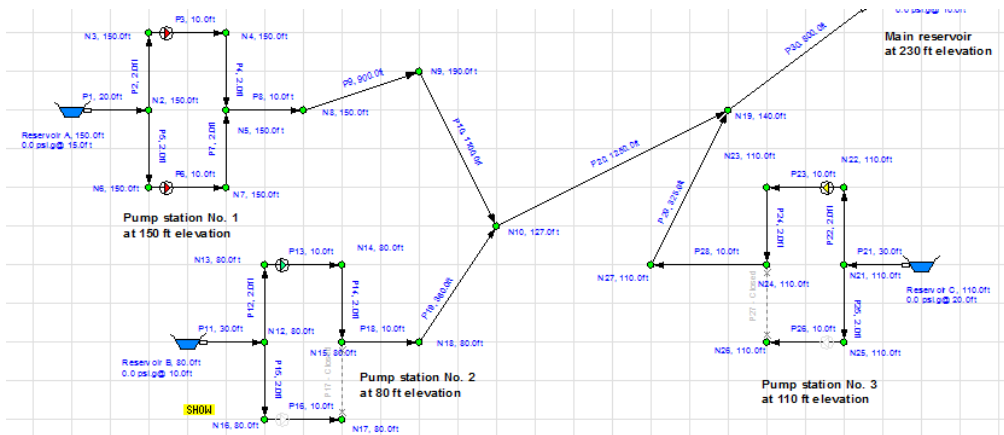


Figure 4-1: Simple hydraulic system skeletonization (Source: pipe flow expert, 2016)

The network to be modelled is re-drawn into the model.

4.3 Hydraulic components

In a hydraulic system/network, there are several components and all these components are modelled in pipe flow expert in somewhat different ways.

4.3.1 Fluid source (tanks or reservoirs):

These are normally used at the start of the system representing the source of the fluid in this case water. The reservoir shape and size don't pose any effect on the system calculations. In usage of a tank, the dimensions are assumed to be infinitely big hence the discharge and inflow quantities don't have to match. The potential energy (PE) of the fluid will be a combination of the surface pressure, elevation and the liquid level which parameters are presented in the boxes on the left hand side of the drawing pane. This PE provides some driving force to the fluid hence creation of flow. Pressure is measured in gauge pressure in bars (bar. g) equivalent to 10m head.

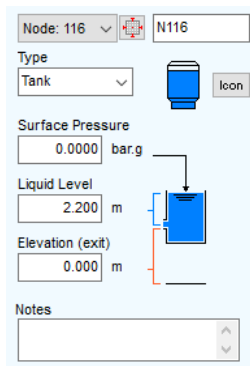



Figure 4-2: Node box

The surface pressure must be set to 0.000 bar.g when the fluid in the tank is open to the atmosphere otherwise, for pressurized tanks, the pressure in the tank must be presented.

The pressure at the entry to the pipe system is calculated basing on the parameters; outlet elevation, liquid level, surface pressure and the density of the liquid.

Note that pipes that connect the same tank must be of the same fluid zone.

4.3.2 Nodes

A node  is a point where two or more pipes meet. Nodes are of three categories, tank, end pressure, and join point. They are used to specify the starting and ending elevations of the pipe connected. Depending on their purpose, they are named as N1, N2...N116, if they are of joining purpose. If used as end pressure nodes, then the exit flowrate is to be calculated when elevation and pressure are specified. If the pipe has an open ending, then a K-factor of, 1, is given representative of exit losses. Pipe flow has a fitting named 'open pipe exit'

4.3.3 Valves and fittings

Valves and fittings affect the flow of fluids in the pipe therefore, if available

in the system they must be modelled in relation with the appropriate pipe. Fittings and valves have K-factors and the software has a database of these components with standard loss coefficient values from manufacturer catalogues. The model also has a K-factor calculator for losses in rounded entrances, gradual enlargement & contraction, sudden enlargement & contraction, and long pipe bend. There is also a provision of creating new fittings and saving them to the database for future use by the modeler.

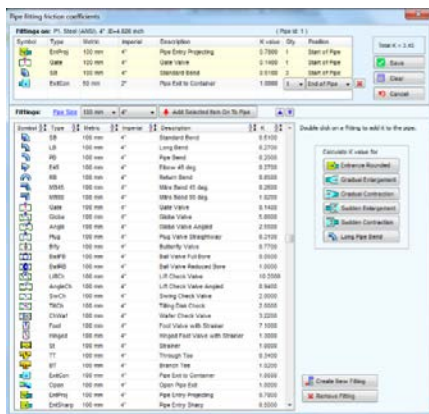
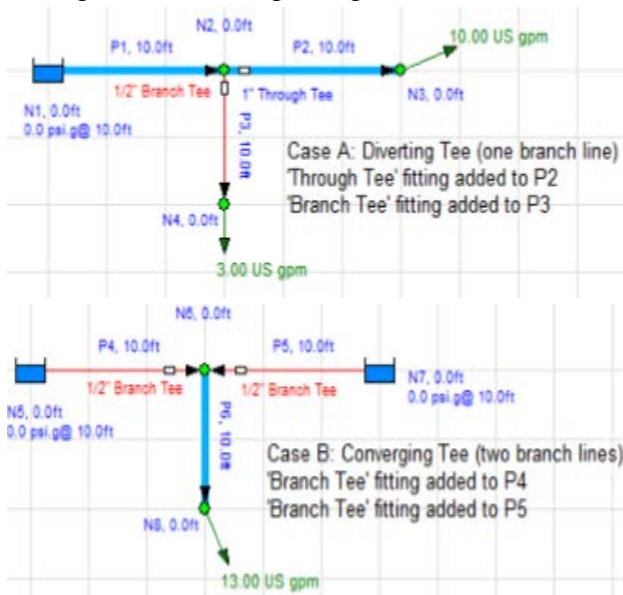


Figure 4-3: pipe fitting friction coefficient

For every fitting chosen from the database, it can be placed either at the start or the end of the pipe during modelling. All fittings that are manually put by the modeler into the model not from the inbuilt database are taken to be bespoke fittings by the software and must match in size with the pipes onto which they are installed.

For the bends; in cases where two pipes are joined by a bend then, the fitting must be put at the end or the start of any of the pipes respectively. The software has all bends included in the database.

Tee fittings: these are treated in a very special manner because flow is different for whatever flow path through the fitting. In this scenario, two fittings are used to describe flow through a tee fitting one at each flow path; “through tee” and “branch tee” where the summation of the losses in each gives the total loss through the tee fitting being modelled.



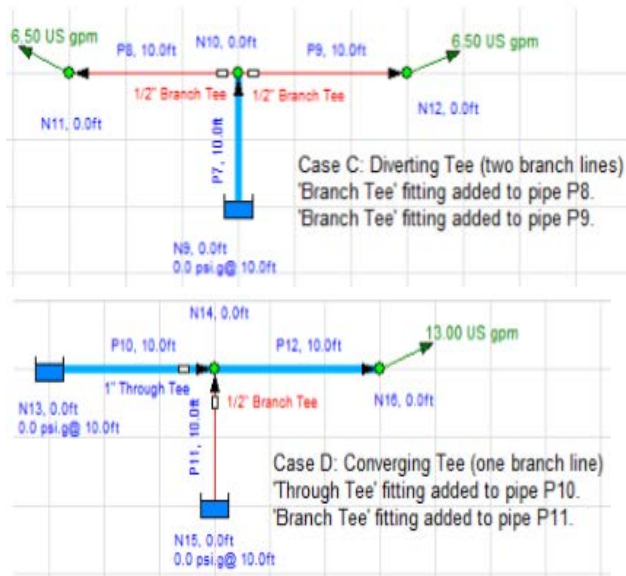


Figure 4-4: Flow paths through tee fittings (Pipe Flow Expert, 2016)

Flow in a tee fitting is of four cases (A, B, C & D) as illustrated in figure 4-4 above representing diverting tee (one branch line), converging tee (two branch lines), diverting tee (two branch lines) and converging tee (one branch line) respectively. In case of un-equal pipe sizes, the fittings associated to that branch line must be of that pipe lines diameter.

4.3.4 Entry and exit losses:

These are also modelled as elements in the system. The software has in its database these losses catered for and the entry losses from the tank into the pipe are of several categories depending on the type of connection to the tank. Re-entrant or protruding connections into the tank, rounded, sharp edged entrances have their K-values included as 0.78 and 0.5 for re-entrant and sharp edged entrances respectively. More information is available in the pipe flow expert user guide.

4.3.5 Components

There are many other elements that are not available in the model software database which the user would like to incorporate in the system. These elements can be modeled as customized elements also known as bespoke

fittings in the system. Some of these components may include but not limited to flow control valves (FCV), filtration systems, flow meters, and any other element that causes a resistance to flow in the system. Pressure losses in these elements can be represented as;

1. Fixed loss representative of the total measured loss through the component
2. Curve loss where a number of values of flow rate (m^3/sec) are plotted against specific head losses (m fluid) generating a curve describing the trend of pressure drop with respect to flow.
3. Manufacturers also publish Cv & Kv flow coefficients to further describe the flow vs pressure drop characteristics of control valves. Cv & Kv coefficients are not the same as the K-factor for standard valves and fittings. Cv & Kv defines the flowrate of a fluid that occurs at a given pressure drop across a component. i.e., Kv is the volume of water in m^3/hour at 20°C with a 1.0 bar pressure drop across the component.

4.4 Solution procedure

Once the system has been schematized, simplified and drawn into the model, the modeler needs to specify certain boundary conditions for the model to run i.e. initial demand in terms of flowrates in and out of the system or pressure. Pipe flow expert then, generates initial flow rate estimates in each pipe following junction continuity at each node (Eqn. 3-4) and the energy loop principle expressed in Eqns. (3-5 and 3-6) in section 3.1.2. The pressure losses are then calculated with in the model using Eqn. (2-20) (Colebrook-White equation) to get the friction factor, f , which is substituted in Eqn. (2-15) (Darcy-Weisbach Equation) for the friction pressure loss of each pipe.

The initial estimates made using the linear theory method don't lead to a balanced pressure result throughout the entire system, so these values are further adjusted using a variation on the Newton method seen in section 3.1.4.2 so as the final result converges to the extent where all the objective functions (flowrate and pressure) within the system balance.

Pipe flow expert defines the several elements of the pipe network or system as a series of highly non-linear matrix equations very difficult or almost impossible to be mathematically/analytically computed. At this point a tentative solution has already been obtained therefore, this result is refined

using Newton method algorithm for mutual convergence of the specified objective function.

The results, as per the need of the modeler, can be viewed on the results drawing and on the results grid.

CASE STUDY SIMULATION

5.1 Simulation of flow in Vombverket hydraulic system

The flow in the hydraulic system at Vombverket was modeled and simulated using the commercial model “pipe flow expert” discussed in chapter 4. From a hydraulic perspective, Vombverket drinking water treatment plant consists of several components that give resistance to the passing flow in the pipelines. The system is a very complex one.



Figure 5-1: Vombverket aerial view

5.2 Vombverket hydraulic system

This hydraulic system is made of reservoirs (tanks), pipes (short length), rapid sand filters, bends, tees, gradual and sudden contraction as well as enlargement fittings, flow meters, flow control valves, hydraulic structures like weirs and venturi-meters. All these elements have been discussed in chapter 2; section 2.3 of this report.

Vombverket hydraulic system layout

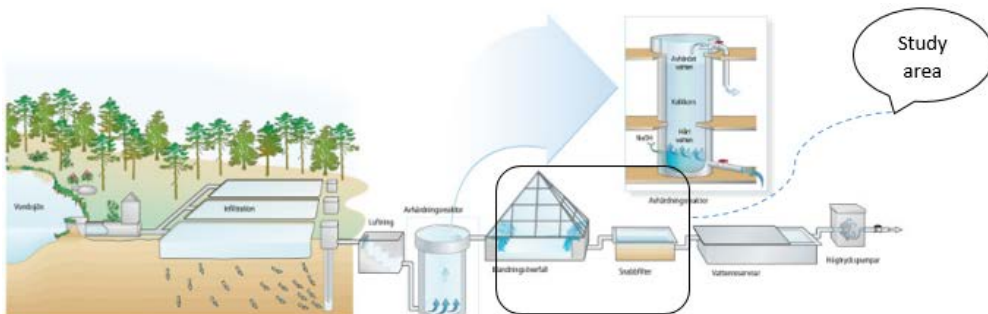


Figure 5-2: Vombverket water treatment plant hydraulic system layout. Study area in fig. 5-5.

This report is focused to modelling the hydraulic system starting from the mixing chamber to the chloramine dosing chamber located between the rapid sand filters and the water reservoir as shown in the box in figure 5-2. A detailed drawing of the study area is given in figure 5-5 later in this chapter.

Pipe flow expert has an elements-database that includes most of the components in the Vombverket hydraulic system.

5.2.1 Bends and bespoke fittings

The treatment plant has three kind of bends; standard, long standard bends and long pipe bends which are modeled.

Standard elbows (bends). 45 degree elbows – these are present in the model database and depending on the diameter a specific *k-value* is assigned. The same applies to the standard 90-degree elbow. The bend fitting is put at the start or end of a pipe with the same diameter. In this model it was assumed that the nominal pipe diameter is equal to the inner pipe diameter.

Long standard bends have their *k-values* provided representative of the pipe diameter. The long pipe bends are considered custom fittings or bespoke fittings whose *k-value* was calculated by inputting the radius of curvature and the pipe diameter. The *r/d* ratio once obtained, the *k-value* can be calculated.

Other fittings considered as bespoke fittings are the sudden and gradual contraction as well as enlargement fittings whose *k-value* was also calculated through the input of the pipe diameter values at both sections of the pipeline together with the length where applicable.

5.2.2 Tees

These are of two types, through and branched tees. They are discussed in details in section 4.3, in this report. They are of convergent and divergent nature.

5.2.3 Pipes

The hydraulic system is sectioned into three parts based on location. There are three filter buildings 1, 2 and 3 which represent the three section of the system for simplification. The pipe material used is cast iron in most of the large diameter pipes in filter building 1 and 2 and stainless steel for some pipes in the filter building 3 and small diameter pipes in buildings 1 and 2. There are a

few pipes connecting the three buildings that are of concrete (SENTAB) material. These concrete pipes were modeled as cast iron pipes because of lack of conclusive information and data about their specifications. The plant has a very complex pipe system but for this project, we only put emphasis on the main water path from the mixer to the disinfection section. The backwashing and drainage sections of the system plus other mini sections were not included in the study because they have no contribution to the flow resistance in the system.

5.2.4 Control valves

The valves in the treatment plant are automated, hence fitted with actuators for accurate and easy control. All these valves are connected to the central control system. The flow in the system is regulated by the percentage of valve opening all depending on the demand. The pressure and flow measurements used in the modeling process were obtained when the valves were both fully and partially open. The types of valves present in the plant's system are; gate valves and butterfly valves.

5.2.5 Tanks (reservoirs)

There are five reservoirs within the project section. These include; the mixer, the two weir basins located at filter building 1 and 2 respectively, the safety basin located in filter building 3 that works as an escape route for water in case the flow at the intake exceeds the filters' capacity. The water will rise and flow over the high wall into the 1600mm pipe connecting to the disinfection basin hence bypassing the filtration process. The model simulation ends in the disinfection basin.

5.2.6 Flow meters

As discussed in chapter two, the flowmeters used at Vombverket are of the electromagnetic type with a very minimal energy loss effect to the system. These are found in all the three filter buildings and one on the final pipeline to the disinfection basin.

There are two Venturi meters in the system. These are really short compressed devices in both filter building 1 and 2. In this projects, these are looked at as one of the major culprits in the energy loss through the system.

5.2.7 Rapid sand filters

There are 26 rapid sand filters in the Vombverket hydraulic system. Filter buildings 1 and 2 have 10 filters in each, with 24 square meters of surface area per filter. Filter building 3 which is the newest of all the buildings and is as a result of the expansion that lead to the energy loss issues has 6 filters of 40 square meters each almost twice the size of the filters in buildings 1 and 2. The filter's sand was replaced in the filter blocks 1 and 2 as well as filter block 3, in 1999. These filters are flushed automatically at specified set periods. The flushing mechanism is not based on the pressure drop across the filters but is soon changed when the pressure gauges are replaced.



Figure 5-3: Schematic diagram of the filter 2. (Persson, T., et al, 2015)

Figure 5-3 represents filter 2 in filter block 1 that has *tritonbottnar* layer and the rest of 25 filters in all the blocks have the same layout. These are similar to the ones available in Ringsjöverket treatment plant but twice bigger – standing at 80 square meters of surface area.



Figure 5-4: Schematic diagram for the 25 filters (Persson, T., et al, 2015)

5.3 Schematization of the system

The Vombverket drinking water treatment plant's hydraulic model was schematized taking to consideration the representation of all the elements that cause major impacts to the flow in the system. The pipes and all the fittings that contribute to the local losses in the system as discussed in section 2.3 were included. The schematized layout is divided into three sections, filter block 1, 2 and 3. These are then joined together with pipes. The system starts in the mixer that is represented as a tank. The elevation, liquid level and surface pressure were the initial standard inputs. The mixer is open to the atmosphere hence the surface pressure of 0.000 bar.g. What to include and exclude depended on the modeler's experience with the system and the literature reviewed. The junctions/nodes are not true physical elements but mark points where two or more pipes or valves are connected. The nodes are connected by links representative of the pipeline. The length, diameter and roughness of the pipe based on the material were the initial standard inputs to the system. The node elevations giving the start and ending elevations of the pipelines also were fed to the model. Depending on the pipe properties and fittings characteristics, the *k-values* were calculated. Reservoirs are nodes that represent an infinite external source or sink of water. There are no pumps in the studied water pathway but there are pumps in the backwash loop.

Some of the elements in the system could not be easily modeled. Therefore, had to be represented/modeled as other components. For-example, *Rapid sand filters* – in filter block 1 and 2 – the sand filters were modeled as system components with energy losses equivalent to that expected through the filters. For a component, pipe flow expert gives options to model the energy losses. This can be as a fixed loss, curve loss or through Kv and Cv coefficients as discussed in chapter 4. For this part of the system the curve loss option was used. Three values of flowrate vs. pressure drop were feed to the model and a second order regression curve generated giving a certain pressure drop at specific flow rate across the filter. The filters in these buildings are assumed to have the same characteristics and properties hence the same curve loss was used in all the 20 filters.

For filter block 3 – the six sand filters are twice as big as those in building 1 and 2. Therefore the flows were doubled across each filter and the three values feed to the model to generate the second order regression curve for these filters.

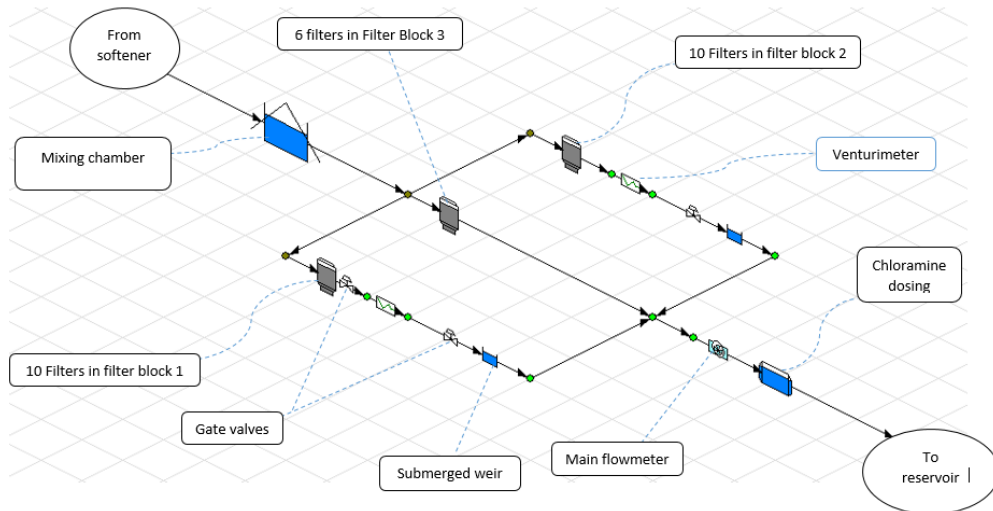


Figure 5-5: Vombverket drinking water treatment plant model simplification

The system layout in the schematic diagram (fig. 5-5), all the elements contributing to the pressure drop in the system are represented.

The Venturi meters were also modeled as component with curve loss. The second order regression curve was generated after the input of flow rate vs. pressure drop values into the model. The three values of flowrate vs head loss were obtained from a series of dataset obtained over a period of 14 days at the plant.

There are two hydraulic structures (weir), one in each of the blocks 1 &2. These weirs become submerged after the expansion of the plant. Their effect is not felt in the system hence making them reservoirs within the flowpaths. The level of water in this tank is assumed constant. The exit losses into the basin and entrance losses into the continuing pipeline are included but not the tank because as discussed earlier in chapter 4, the model treats a tank as an infinite source in which the flow-in doesn't equal to the flow-out. This was creating a disconnection into the system hence neglecting the tank. Some other

connections to the system were closed off thus don't contribute to the calculations.

The valves at Vombverket are most of the time partially open to attain a certain demand yet standard globe or butterfly valves can't be modelled at partial opening. Therefore, FCV were introduced to play the role of the partial opening keeping the flow at set value. This is done during the flow calibration stage to reproduce what is at the plant. Note: *The FCV cannot introduce a negative pressure loss.*

2 (FB-2)

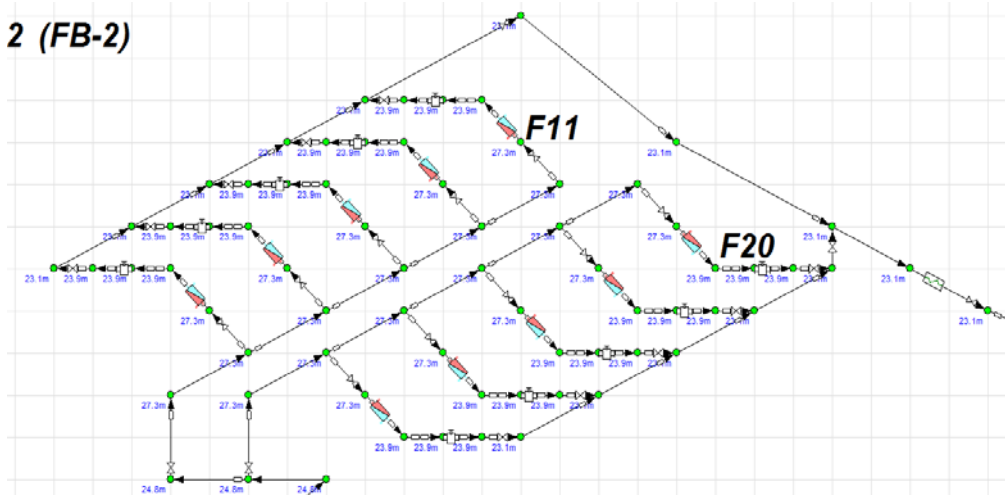


Figure 5-6: FB2 composition and detailed model layout

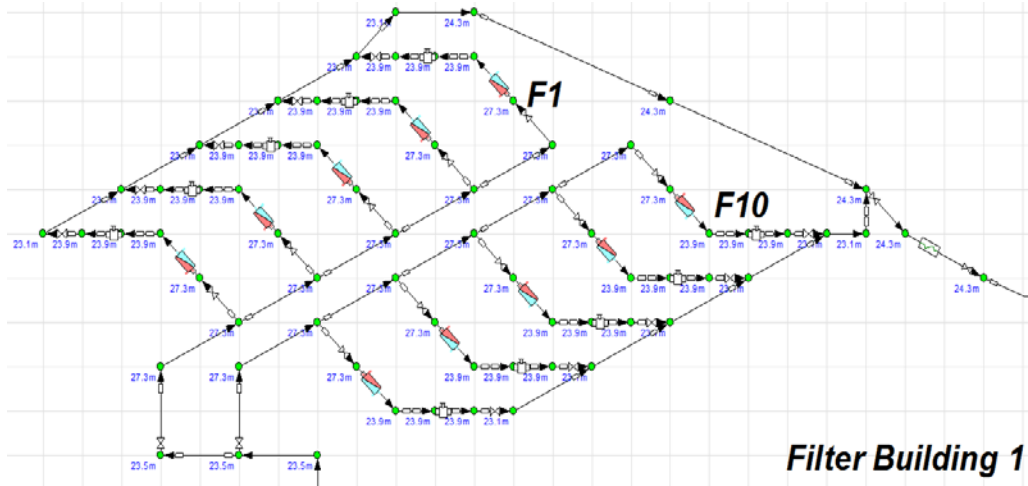


Figure 5-7: FB1 composition and detailed model layout

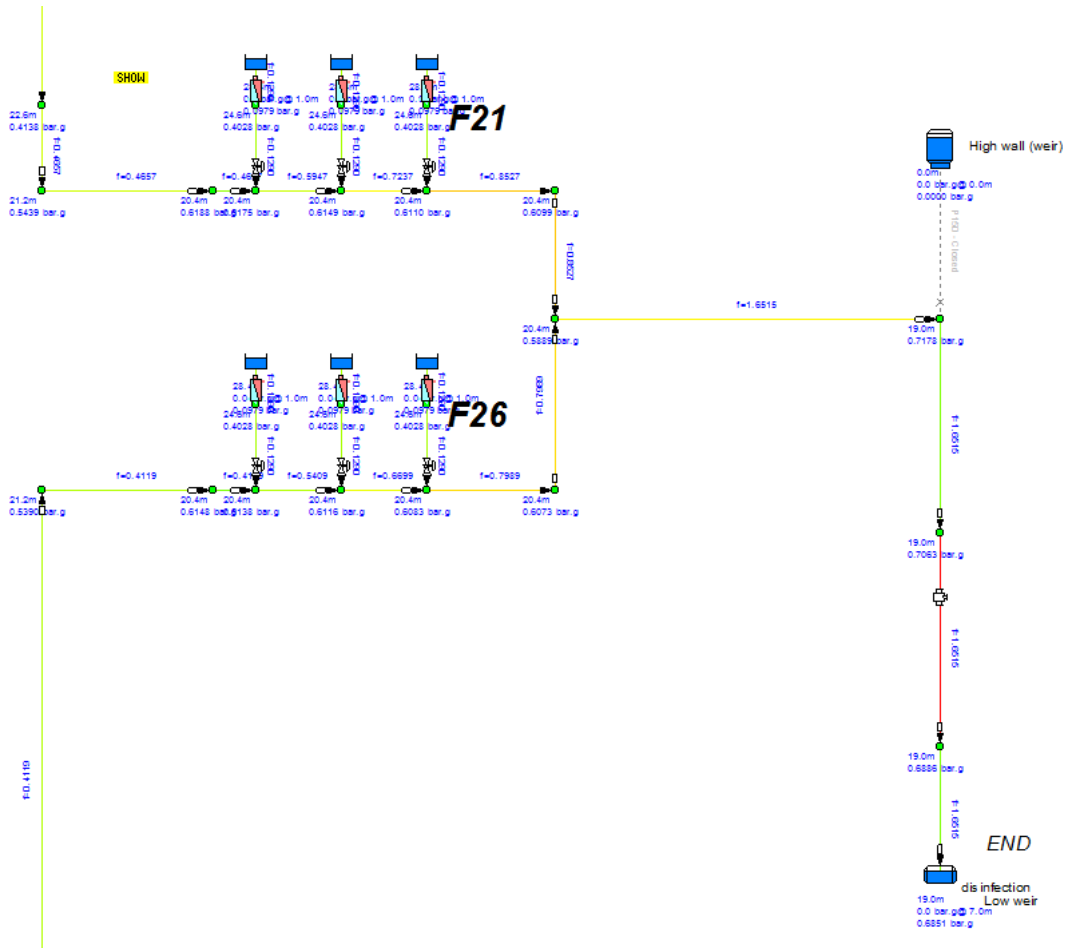


Figure 5-8: Detailed model layout of the filters in FB3

FIELD MEASUREMENTS

6.1 Measured Datasets

Several measurements were obtained to be used to set boundary conditions, system optimization, calibration and validation of the model. These data measurements include;

6.1.1 Pressure at selected points in the system.

Using pressure gauges, relative/gauge pressure was obtained at specific times of the day in all the filter buildings at the plant. For filter buildings 1 and 2, pressure at points near the flow meters from each filter was measured each time recording both gauge pressure and the respective time of the day it's taken. The time was later used to obtain the specific flow at that time through the filter or the node using the system controlling software. See table 6-3

6.1.2 Pressure at the point before the Venturi meter.

The correction distance between the measured points was also measured and recorded.

Table 6-1: Pressure and flowrate measurements from FB1.

| FILTER BUILDING 1 | Pressure measured next to the flow meter at each filter (m) | Pressure drop between the filter and the Venturi (m) | Water flow (l/s) |
|-------------------|---|--|------------------|
| Filter 1 | 3.16 | 0.64 | 54 |
| Filter 2 | 3.19 | 0.67 | 41 |
| Filter 3 | 3.15 | 0.63 | 44 |
| Filter 4 | 3.3 | 0.78 | 37 |
| Filter 5 | 3.34 | 0.82 | 36 |
| Filter 6 | 3.33 | 0.81 | 36 |
| Filter 7 | 3.37 | 0.85 | 38 |
| Filter 8 | 3.36 | 0.84 | 40 |
| Filter 9 | 3.24 | 0.72 | 34 |
| Filter 10 | 3.17 | 0.65 | 49 |

| | | | |
|--------------|--|--|-----|
| Total | | | 409 |
|--------------|--|--|-----|

The measurements are taken in March, 2016(measurements taken by Tobias Persson). Hence,

| | | |
|---|-------|------|
| Height difference between pressure gauges | 0.21 | M |
| Pressure before Venturi meter | 2.73 | M |
| Pressure corrected for height difference | 2.52 | M |
| Conditions | | |
| All valves were fully open | | 100% |
| Start height: (blandningsöverfall) | 28.45 | M |
| End height (Överfall klordosering) | 26.00 | M |

These measurements are representative of the maximum flow through the filters in the present situations at the plant. These flows are below the initial design properties and capacity of the system. The measurements in filter building 1 were obtained on different dates compared to those in block 2 and 3 that were taken on the same date during similar flow conditions. Flushing filters when taking measurements highly affected some of results leading to many repetitions of the exercise.

Table 6-2: Measured values from Vombverket in filter block 2.

| FILTER BUILDING 2 | Pressure measured next to the flow meter at each filter (m) | Time (am) | Pressure drop between the filter and the Venturimeter (m) | Water flow (l/s) |
|-------------------|---|-----------|---|------------------|
| Filter 11 | 3.37 | 10:35 | 0.41 | 55 |
| Filter 12 | 3.35 | 8:38 | 0.43 | 46 |
| Filter 13 | 3.37 | 8:50 | 0.41 | 45 |
| Filter 14 | 3.36 | 8:59 | 0.42 | 43 |
| Filter 15 | 3.37 | 9:06 | 0.41 | 42 |
| Filter 16 | 3.59 | 10:44 | 0.19 | 44 |
| Filter 17 | 3.53 | 9:24 | 0.25 | 46 |
| Filter 18 | 3.5 | 9:35 | 0.28 | 48 |
| Filter 19 | 3.42 | 9:45 | 0.36 | 48 |
| Filter 20 | 3.43 | 9:57 | 0.35 | 58 |

The measurements were taken at approximately similar times window and the flow properties were assumed to be the same (as measured by the modeler on 13th -4-2016). Therefore,

| | | |
|---|------------------|-----------------|
| Height difference between pressure gauges | 0.844 | M |
| Pressure before Venturi meter | 3.78 | <i>m</i> 9:55am |
| Pressure corrected for height difference | 2.936 | <i>M</i> |
| Conditions | | |
| All valves were fully open | <i>100% open</i> | |

The corresponding flowrates through each filter in the entire system at the time the pressure reading was picked are shown below in table 6-3. With this, the pressure values measured can easily be analyzed and compared to the calculated values by the model hence validation of the model performance.

Table 6-3: Flow results at specified times of the day when pressure readings in FB2.

| Time | F1 | F2 | F3 | F4 | F5 | F6 | F7 | F8 | F9 | F10 | F11 | F12 | F13 | F14 | F15 | F16 | F17 | F18 | F19 | F20 | F21 | F22 | F23 | F24 | F25 | F26 |
|-------|----|----|----|----|----|----|----|----|----|-----|-----|-----|-----|-----|-----|-----|-----|-----|-----|-----|-----|-----|-----|-----|-----|-----|
| 8:38 | 32 | 32 | 32 | 32 | 32 | 32 | 32 | 32 | 29 | 32 | 55 | 47 | 45 | 42 | 42 | 43 | 46 | 49 | 48 | 56 | 80 | 78 | 80 | 80 | 79 | 79 |
| 8:50 | 33 | 33 | 33 | 32 | 32 | 33 | 33 | 32 | 32 | 32 | 55 | 46 | 45 | 42 | 42 | 44 | 46 | 49 | 48 | 56 | 81 | 81 | 81 | 81 | 81 | 80 |
| 8:59 | 28 | 0 | 30 | 30 | 30 | 30 | 30 | 29 | 36 | 29 | 55 | 47 | 45 | 43 | 42 | 44 | 46 | 49 | 49 | 56 | 69 | 71 | 69 | 71 | 70 | 71 |
| 9:06 | 28 | 0 | 27 | 28 | 30 | 30 | 29 | 30 | 33 | 28 | 55 | 47 | 45 | 43 | 42 | 44 | 46 | 49 | 48 | 56 | 73 | 75 | 74 | 74 | 75 | 76 |
| 9:24 | 29 | 29 | 30 | 30 | 29 | 29 | 29 | 29 | 28 | 29 | 55 | 46 | 45 | 43 | 42 | 44 | 46 | 49 | 48 | 56 | 73 | 75 | 73 | 74 | 74 | 73 |
| 9:35 | 32 | 33 | 31 | 33 | 33 | 33 | 32 | 33 | 26 | 33 | 54 | 46 | 44 | 42 | 41 | 43 | 46 | 48 | 48 | 56 | 81 | 83 | 83 | 81 | 82 | 82 |
| 9:45 | 32 | 33 | 33 | 32 | 33 | 32 | 32 | 32 | 32 | 32 | 54 | 46 | 45 | 42 | 41 | 43 | 46 | 48 | 48 | 56 | 80 | 80 | 81 | 82 | 81 | 81 |
| 9:55 | 32 | 32 | 32 | 32 | 32 | 32 | 32 | 31 | 32 | 32 | 61 | 0 | 53 | 50 | 48 | 45 | 48 | 50 | 50 | 58 | 79 | 79 | 78 | 78 | 79 | 80 |
| 9:57 | 32 | 32 | 32 | 32 | 32 | 32 | 32 | 31 | 31 | 31 | 61 | 0 | 54 | 50 | 48 | 46 | 48 | 50 | 50 | 59 | 76 | 77 | 77 | 76 | 76 | 76 |
| 10:35 | 28 | 28 | 28 | 28 | 29 | 28 | 28 | 28 | 28 | 28 | 55 | 51 | 44 | 42 | 41 | 43 | 45 | 48 | 47 | 55 | 24 | 72 | 72 | 69 | 69 | 69 |
| 10:44 | 30 | 31 | 31 | 30 | 30 | 30 | 31 | 31 | 27 | 30 | 55 | 51 | 45 | 42 | 41 | 43 | 46 | 48 | 48 | 55 | 0 | 76 | 77 | 79 | 77 | 77 |

The values in red represent the scenario where there was no filter back-washing at the time of the pressure reading. As of 13th -4-2016. This dataset was used for validation of the model. Specific sensitive pressure points were chosen for filter building 3. These included the big tee junction where the water from filter buildings 1, 2 and 3 meets in a pipe of 1200mm inner diameter. This is also expected to be one of the major culprits responsible for the energy drop in the system.

Table 6-4: Measured values from Vombverket in FB3.

| FILTER BUILDING 3 | | Pressure gauge reading at point next to the flow meter at each filter (m) | | Elevation from set level | unit s |
|-----------------------------|------|---|--|--------------------------|--------|
| Filter 21 | 4.5 | M | | 0.065 | m |
| Filter 26 | 4.6 | M | | 0.090 | m |
| | | | | | |
| Big tee junction (1200mm) | 4.7 | M | | 0.075 | m |
| Point at the main flowmeter | 3.26 | m | | 1.20 | m |

The measurements are taken within similar times of the day and the flow properties are assumed to be the same (as measured by the modeler). Some datasets were obtained from 18th –June-2014 at 21:00 mid-summer night when the plant recorded the highest flow shown in table 6-5 below

Table 6-5: Dataset for midsummer 2014 at 21:00 (from control system archives)

| Filter block 1 | | Filter block 2 | | Filter block 3 | | Units |
|----------------|---------|----------------|----|----------------|----------------|-------|
| F1 | 54 | F11 | 52 | F21 | 130 | l/s |
| F2 | 41 | F12 | 49 | F22 | 128 | l/s |
| F3 | 44 | F13 | 47 | F23 | 129 | l/s |
| F4 | 37 | F14 | 40 | F24 | 129 | l/s |
| F5 | 36 | F15 | 40 | F25 | 129 | l/s |
| F6 | 36 | F16 | 43 | F26 | 130 | l/s |
| F7 | 38 | F17 | 47 | | Average 129 | l/s |
| F8 | 40 | F18 | 48 | | | l/s |
| F9 | 34 - 39 | F19 | 48 | | | l/s |
| F10 | 49 | F20 | 55 | | | l/s |

Measurements were also taken at the venturi meter in filter building 1 since here we have two pressure gauge connection points. One just before the device and the other below the weir basin. The weir at this point is submerged hence this gauge will measure the static pressure representative of the pressure after the venturi meter. Values of head loss vs. flowrate at this location were obtained for the period between 10/1/2015 at 00:00 to 10/14/2015 at 00:00 for every 6 minute. This gave a very good dataset across the venturi meter over this time giving a proper analysis behavior of the system. The values obtained are used to plot a second order regression curve (polynomial) of head loss against flowrate getting the best fit curve over the dataset. From this best fit, the equation of the curve is obtained and used to get the three points needed in the model to generate a second order curve over which the model will calculate the head losses with respect to the flowrate through the Venturi.

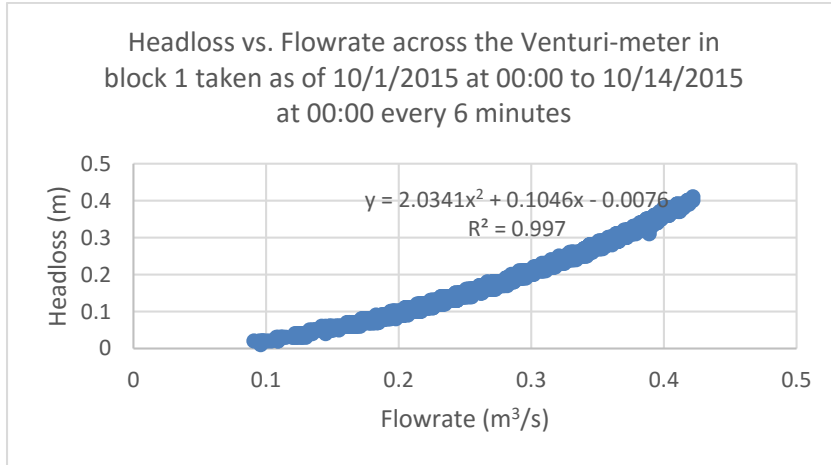


Figure 6-1: Second order curve across the venturi meter in FB1 (Dataset from system archives).

$$H_l = 2.0341Q^2 + 0.1046Q - 0.0076 \quad (6-1)$$

For $Q = 0$, $H_l \approx 0$. When $Q = 0.5 \text{ m}^3/\text{s}$, $H_l = 0.56 \text{ m}$ and at $Q = 0.3 \text{ m}^3/\text{s}$, $H_l = 0.21 \text{ m}$

Equation 6-1 is a second order regression curve equation governed by the model software. All the data for head loss in m is plotted against flow rate Q (m^3/s) as obtained from the measurements across the venturi.

Theoretically we would expect to have equation 6-1 similar to equation 2-22 expressed in terms of flowrate in square (Q^2).

$$h_l = \frac{KQ^2}{2gA^2} = CQ^2 \quad (6-2)$$

This is not considered since the model will only use the second order curve equation that it generates using three points obtained from equation 6-1. See figure 6-2.

Table 6-6: Calculated values of flowrate vs. head loss as obtained from the curve equation in fig. 6-1

| Flowrate (m^3/s) | Head loss (m) |
|------------------------------------|---------------|
| 0 | 0 |
| 0.3 | 0.21 |
| 0.5 | 0.56 |

These three coordinates in table 6-6, are entered into the model to generate a second order curve loss across the venturi meter.

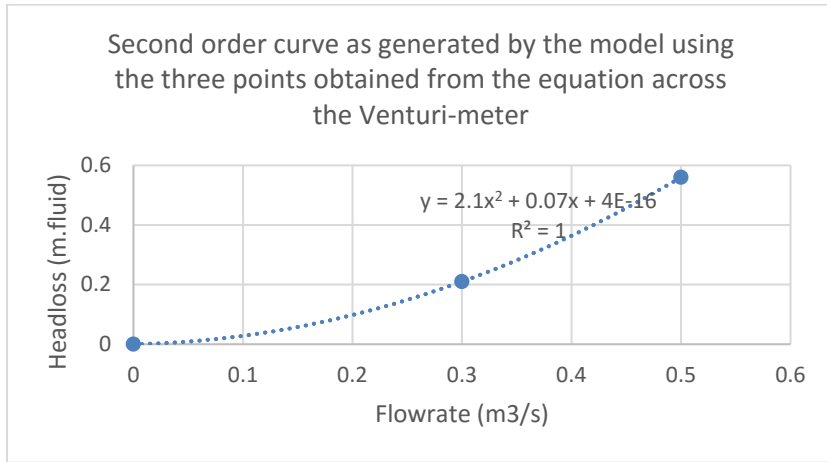


Figure 6-2: Second order curve across the venturi meter in FB1 (model)

For measurement of flowrate against head loss across the rapid sand filters in block 1 and 2, three points are feed to the model generating a second order polynomial representative of the pressure drop behavior across the filters at specific flowrates

Table 6-7: Flow measurements vs. head loss across the rapid sand filter in block 1 and 2

| Flow rate (m ³ /s) | Head loss (m) |
|-------------------------------|---------------|
| 0 | 0 |
| 0.032 | 0.26 |
| 0.037 | 0.31 |

Therefore, once fed into the model;

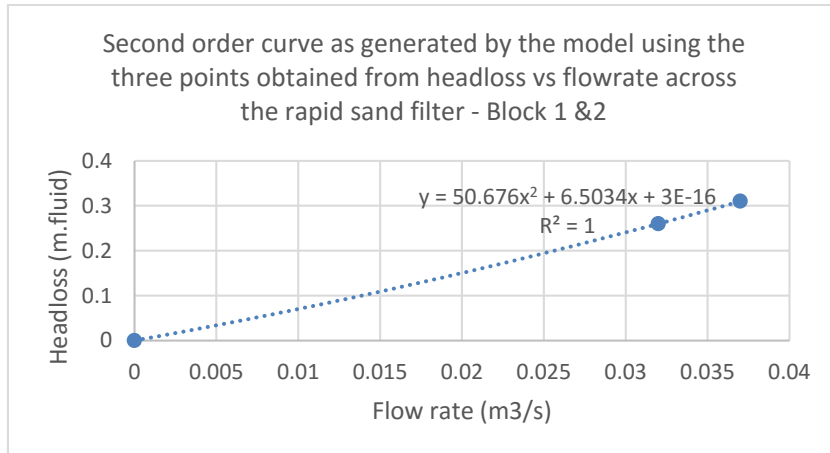


Figure 6-3: Second order curve for filters in block 1 and 2 as generated by the model

For filter block 3 - Since the filter surface area is approximately twice the size of those in block 1 and 2, the flowrate was doubled but at the same head loss. The assumption is that, there exists similar conditions and characteristic in the filter materials.

Table 6-8: Flow measurements vs. head loss across the rapid sand filter in block 3

| Flow rate (m ³ /s) | Head loss (m) |
|-------------------------------|---------------|
| 0 | 0 |
| 0.064 | 0.26 |
| 0.074 | 0.31 |

Therefore, once fed in the model;

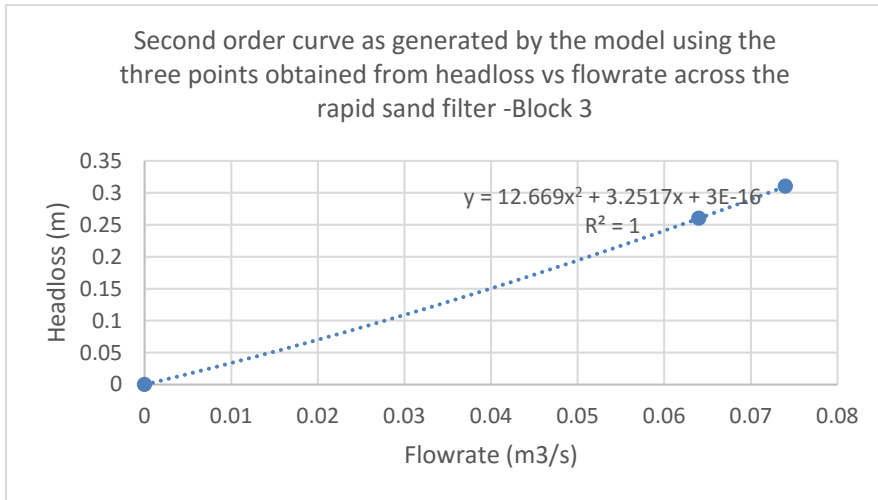


Figure 6-4: Second order curve for filters in block 3 as generated by the model

In filter block 3, the flow from each filter is controlled by flow control valves. The flow control valve introduces an additional head loss in the network to ensure that the flow is maintained to a value specified by the modeler. The added head loss is reported in the results table. The maximum allowed flow from each of these filters is 129 l/s as of now but they can give more than that. While in filter block 3, measurements of pressure at specific points were obtained similar to the ones shown earlier in table 6-3 above at slightly different times of the day since the modeler had limited number of gauges and man-power.

Starting from 13:50pm to 14:49pm of April 13th 2016, the modeler obtained gauge pressure value as shown in the tables below. The respective flowrates from filter blocks1 and 2, and flow from each of the six filters in block 3 was obtained from the control system archives. These are given in the table below,

Table 6-9: Modeler's measurements at 13:50pm at Filter 26 (F26)

| Time | FB1 (l/s) | FB2 (l/s) | F21 (l/s) | F22 (l/s) | F23 (l/s) | F24 (l/s) | F25 (l/s) | F26 (l/s) |
|--------------------------|--------------|--------------|--------------|--------------|--------------|--------------|--------------|-----------|
| 13:50pm | 320 | 296 | 72 | 72 | 71 | 73 | 73 | 73 |
| Measured pressure at F26 | | | | | | | | 0.57bar.g |

where FB represents Filter Block and F represent Filter name.

Table 6-10: Modeler's measurements at 14:06pm at Tee Junction

| Time | FB1 (l/s) | FB2 (l/s) | F21 (l/s) | F22 (l/s) | F23 (l/s) | F24 (l/s) | F25 (l/s) | F26 (l/s) |
|-----------------------------------|--------------|--------------|--------------|--------------|--------------|--------------|--------------|------------|
| 14:06pm | 315 | 276 | 67 | 67 | 67 | 67 | 66 | 67 |
| Measured pressure at Tee Junction | | | | | | | | 0.565bar.g |

Table 6-11: Modeler's measurements at 14:18pm at Filter 21 (F21)

| Time | FB1 (l/s) | FB2 (l/s) | F21 (l/s) | F22 (l/s) | F23 (l/s) | F24 (l/s) | F25 (l/s) | F26 (l/s) |
|--------------------------|--------------|--------------|--------------|--------------|--------------|--------------|--------------|------------|
| 14:18pm | 290 | 280 | 64 | 64 | 65 | 64 | 63 | 66 |
| Measured pressure at F21 | | | | | | | | 0.535bar.g |

Another measurement was taken at the main flow meter towards the end of the study portion of the system.

Note, F1 to F10 are in filter block 1, F11 to F20 in filter block 2 and F21 to F26 are in filter block 3.

Table 6-12: Modeler's measurements at 14:49pm at main flowmeter

| Measurement /Time | Point | Flowrate (l/s) | Measured Pressure (bar.g) |
|---------------------------|-------|----------------|---------------------------|
| Main flowmeter 14:49pm | - | 992 | 0.576 |

RESULTS

7.1 Simulation Results

The system schematization was drawn into the model. The drawing need not to be on scale, the data values entered are the ones that will be used for the calculations. Input all the pipe features together with the fittings associated. After all the components were fitted into the model and the necessary boundary conditions set, the model was run.

7.2 Existing system

The dataset in table 7-1 was used to check the model getting an approximate comparison of the system results to the actual measured results at the plant. This dataset is for results when the plant was run at full capacity with all the valves were 100% open on mid-summer of 2014.

Table 7-1: Comparison of measured Vs. Model results for midsummer of 2014

| Filter (FB1) | Measured (l/s) | Cal c. (PFE) | Filter (FB2) | Measured (l/s) | Cal c. (PFE) | Filter (FB3) | Measured (l/s) | Cal c. (PFE) | units |
|--------------|----------------|--------------|--------------|----------------|--------------|--------------|----------------|--------------|-------|
| F1 | 54 | 42 | F11 | 52 | 45.6 | F21 | 130 | 129 | l/s |
| F2 | 41 | 40.6 | F12 | 49 | 44.5 | F22 | 128 | 129 | l/s |
| F3 | 44 | 39.8 | F13 | 47 | 44.2 | F23 | 129 | 129 | l/s |
| F4 | 37 | 40.5 | F14 | 40 | 44.4 | F24 | 129 | 129 | l/s |
| F5 | 36 | 41.7 | F15 | 40 | 45.2 | F25 | 129 | 129 | l/s |
| F6 | 36 | 42.2 | F16 | 43 | 44.4 | F26 | 130 | 129 | l/s |
| F7 | 38 | 41 | F17 | 47 | 43.6 | | | | l/s |
| F8 | 40 | 40.3 | F18 | 48 | 43.4 | | | | l/s |
| F9 | 39 | 41.2 | F19 | 48 | 43.7 | | | | l/s |
| F10 | 49 | 42.6 | F20 | 55 | 44.7 | | | | l/s |
| TOTAL | 414 | 412 | | 469 | 444 | | 775 | 774 | l/s |

On the first attempt to run the model, calculated results (calc.) by the model in filter block 1 are seen to be in agreement with the measured results. The model results in block 2 however, are not in expected agreement with the measured data at the plant.

7.2.1 Sensitivity Analysis

This process involved identification of those parameters in the system design that the model was most sensitive to (Da Silva et al, 2015). Determination of the degree of sensitivity or the impact caused to the system when that specific parameter was varied. Evaluation of the way in which adjusting the value (s) of a parameter affected the model output was made, in order to identify parameters that might improve the performance and characteristics of the model. The objective functions include flowrate (m^3/s) and head losses (m).

The parameters that were evaluated include, node elevation, liquid levels, element *k-value*, bespoke components' characteristics (curve loss), pipe inner diameter and pipe length, pipe roughness (mm). The variables that whose sensitivity is being determined or sought is the dependent variable of the objective function and in most cases it's one though it can be more like in this situation they are two pressure and flow rate. The variables whose change or adjustment will improve the performance and characteristics of the model is the independent variable.

Some of these parameters have set/fixed values for this project and their adjustment are not required like the pipe diameter and length. Node elevations, bespoke components' characteristics (curve loss), and liquid levels gave the highest degree of sensitivity and were to be given more attention than others during calibration. The *k-value* for the fittings in the system seemed to be a very sensitive parameter tot the system but the challenge was that, most of the fittings are standard fittings obtained from the model database (manufacturer catalogues) and are given no option to change. The bespoke fittings' *k-values* were calculated using pipe diameter and lengths that are fixed as per the plant specifications hence couldn't be altered.

Note that, the degree of sensitivity assignment is subjective but for this project the parameters to which the model was considered to be sensitive are those that gave an average percentage variation of objective functions' value greater than

5%. The parameters that were considered for adjustment during calibration include, bespoke components' characteristics (curve loss) and node elevation.

7.2.2 Calibration

Data for flowrate vs. head loss was obtained from the control system archive across the filters in filter building 2. This dataset is then used to generate an equation from which a set of three coordinated are obtained. The most perfectly fitting set is given in table 7-2 below. The function to adjust in this calibration was the filter curve loss

Table 7-2: Dataset for calibration of filters in filter building 2

| Flowrate (m ³ /s) | Head loss (m) |
|------------------------------|---------------|
| 0.000 | 0.00 |
| 0.021 | 0.11 |
| 0.029 | 0.13 |
| 0.037 | 0.17 |
| 0.042 | 0.20 |
| 0.042 | 0.21 |
| 0.045 | 0.21 |
| 0.046 | 0.23 |

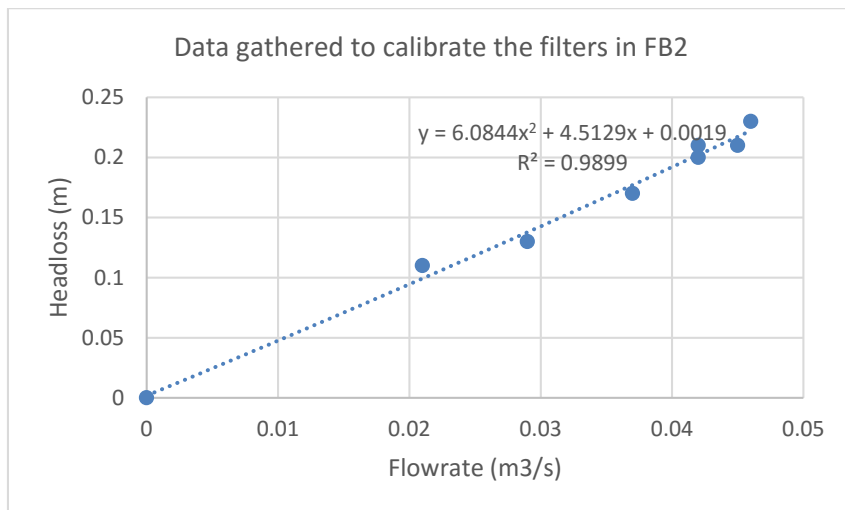


Figure 7-1: Second order curve loss for the dataset in table 7-2.

From the curve equation in fig. 7-1, the three points below are obtained.

Table 7-3: The new points fed to the model to generate the second order curve for the filters in FB2

| | |
|------------------------------|---------------|
| Flowrate (m ³ /s) | Head loss (m) |
| 0.000 | 0.0000 |
| 0.037 | 0.1770 |
| 0.046 | 0.2224 |

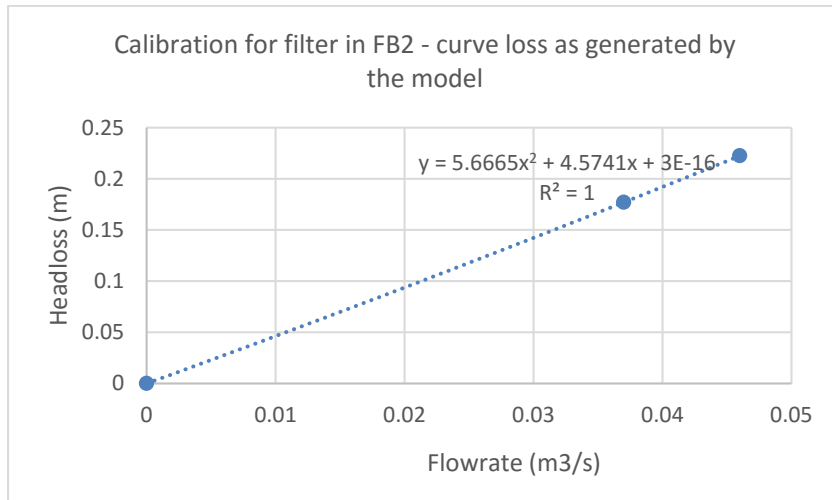


Figure 7-2: New second order curve loss generated in the model

Therefore, the results in table 7-1 are updated to a new matching results after running the model with new values for the curve loss.

Table 7-4: Measured vs. model results after calibration of FB 2

| Filter (FB1) | Measured (l/s) | Calc. (l/s) | Filter (FB2) | Measured (l/s) | Calc. (l/s) | Filter (FB3) | Measured (l/s) | Calc. (l/s) |
|--------------|----------------|-------------|--------------|----------------|-------------|--------------|----------------|-------------|
| F1 | 54 | 42.0 | F11 | 52 | 48.3 | F21 | 130 | 129 |
| F2 | 41 | 40.6 | F12 | 49 | 46.7 | F22 | 128 | 129 |
| F3 | 44 | 39.8 | F13 | 47 | 46.3 | F23 | 129 | 129 |
| F4 | 37 | 40.5 | F14 | 40 | 46.5 | F24 | 129 | 129 |
| F5 | 36 | 41.7 | F15 | 40 | 47.7 | F25 | 129 | 129 |
| F6 | 36 | 42.2 | F16 | 43 | 46.7 | F26 | 130 | 129 |
| F7 | 38 | 41.0 | F17 | 47 | 45.5 | | | |

| | | | | | | | | |
|--------------|-----|--------------|-----|-----|-------------|--|-----|------------|
| F8 | 40 | 40.3 | F18 | 48 | 45.2 | | | |
| F9 | 39 | 41.2 | F19 | 48 | 45.7 | | | |
| F10 | 49 | 42.5 | F20 | 55 | 47.2 | | | |
| TOTAL | 414 | 411.9 | | 469 | 466 | | 775 | 774 |

Therefore, it can be clearly observed that the Model/calculated (calc.) results by pipe flow expert are in agreement with the measured results. The average percentage of variation for the measured and model flowrate results in block 1 is 0.8% (A) and that in block 2 is 0.64% (A) which are overall below 1%. Some of the values especially F1, F10, F11 and F20, seem to be a bit higher than the calculated ones. This is proof that the degree of clogging of the filters varies from filter to filter, it's not the same as assumed in the modeling process.

7.2.3 Validation

The data obtained on 13th April 2016 in tables 6-2, 6-3, 6-9 to 12 was used to validate the model. This involved running the model for each dataset with reference to time of the day. That is to say the model was run for 15 sets.

The table below exhibits the comparison for agreement between the model results and the measured results from Vombverket.

Table 7-5: Validation of Pipe Flow Expert Model in FB2

| Filter | Time | Measured Results (m) | Model Results (m) | Variation % | Remarks |
|--------|---------|----------------------|-------------------|-------------|---------|
| F12 | 8:38 am | 4.194 | 4.198 | 0.095 | A |
| F13 | 8:50 am | 4.214 | 4.224 | 0.237 | A |
| F14 | 8:59 am | 4.204 | 4.186 | 0.428 | A |
| F15 | 9:06 am | 4.214 | 4.208 | 0.142 | A |
| F17 | 9:24 am | 4.374 | 4.222 | 3.475 | D |

| | | | | | |
|---------|-------------|-------|-------|-------|---|
| F18 | 9:35 am | 4.344 | 4.226 | 2.716 | C |
| F19 | 9:45 am | 4.264 | 4.207 | 1.337 | B |
| F20 | 9:57 am | 4.274 | 4.164 | 2.574 | C |
| F11 | 10:35 am | 4.214 | 4.088 | 2.990 | C |
| F16 | 10:44 am | 4.434 | 4.189 | 5.525 | D |
| Venturi | 9:55 am | 3.780 | 4.061 | 7.434 | D |

Legend:

A – variation < 1% = strong agreement

B - variation between 1-2% = Agreement

C - variation between 2-3% = Fair Agreement

D – variation >3% = Disagreement

Another set of data was used by picking random points in other parts of the hydraulic system at different time periods but on the same day to clearly evaluate the performance of the model.

Table 7-6: Validation of the model using extra data from random parts of the system

| Filter No. | Time | Measured Results | Model Results | Variation % | Remarks |
|------------------|-------------|------------------|---------------|-------------|---------|
| F26 | 13:50 pm | 5.70 | 5.707 | 0.123 | A |
| Big-Tee junction | 14:06 pm | 5.65 | 5.598 | 0.920 | A |
| F21 | 14:18 pm | 5.35 | 5.655 | 5.7 | D |
| Main Flowmeter | 14:49 pm | 5.76 | 6.928 | 20.3 | D |

The results that disagree (D) are as a result of the following factors:

1. Measured data obtained just before and after a filter backwashing process. This leaves a transient condition into the system most especially; the backwash pumps that are connected near the big tee junction directly to the system in filter building 3.
2. The unknown degree of pipe roughness (mm) especially in the cast iron pipes. Some of these pipes and fittings were installed in the early 50's and are still operational till now. These provide a very high roughness height (relative roughness) in the system but its unfortunate that such a factor is very difficult to be completely modeled.
3. The presence of concrete pipes (SENTAB) in the system that were not considered in the model because of unknown or limited information about them. This would make it very difficult for them to be modeled hence they were replaced by cast iron in the model.
4. The aspect of human errors during data collection and measurement at the plant. This is in one way a source of the variations in the results.
5. It was also tricky to model the airlocks in the system and the turbulence due to suction of air in the system at the point where the 700mm pipe leave the mixing chamber. This also provides an error percentage in the measurements leading to variations.
6. The 20.3% variation between measured and model results is as a result of the problematic determination of the height for this gauge. It was finally put on a $\frac{3}{4}$ inch pipe more than two meters long and more than 1.2meters elevation from the center of the junction

Overall, the model was considered perfect and valid because it had managed to reproduce the measured results perfectly.

MEASURES

8.1 Measures to reduce energy losses

Firstly, is the identification of the major components that significantly contribute to the system pressure losses. These are shown in the model layout results by the color pattern that depicts the water velocity, see figure 8-1 below. It is noted that the higher the velocity of water the higher the energy losses hence the red coloring represents any velocities above 2.1m/s, orange for velocities between 1.7 – 2.1 m/s, yellowish 1.2-1.7 m/s, light green 0.7 – 1.2 m/s and <0.7 is green. It is observed that in all areas in the model where the velocity is above 1.2 m/s, the energy loss is so high hence a check must be done and any component that might be the possible cause of this resistance must be investigated.

The components investigated in this study include;

1. The Venturi meters in both filter blocks 1 and 2.
2. The gate valve placed before the Venturi meter in FB1.
3. The double bends in filter block 1 that lead to a change in elevation from 23.15m to 24.327m. The effect of this is explained in chapter 2 of this report.
4. The hydraulic structures at the end of the building 1 and 2. These are as of now no longer working as they were designed to. They are completely submerged hence acting as inline tanks in the system. These accumulate an array of losses in the system, like; exit and entrance losses and loss of kinetic energy in flow
5. The Turbulence at the mixing chamber as water joins the pipe system. There is a high suction of air in the system which air has nowhere it escapes from thus taking the same water pathway to the sand filters. This generates a lot of resistance in the system due to the air locks and air pockets created in the pipeline.
6. The 1200mm 90-degree convergent tee junction in filter building 3. This is a point where water from filter block 1 and 2 meet at a converging through tee and leave through the branch. There is a lot of energy lost.

7. The two 800mm 90-degree bends in block 3 leading the water to the 90-degree Tee junction.
8. The constriction from 1600mm to 900mm for the flow meter towards the disinfection basin in block 3. This is where we have the highest pressure drop in the system.

It was impossible to model some of these components like Turbulence and the air pockets in the pipeline. The rest of the components' effect is clearly visible in the model results. The system lay out as produced by the model is shown below (figure 8-1) with all the coloring for clear visibility of the water velocity trend.

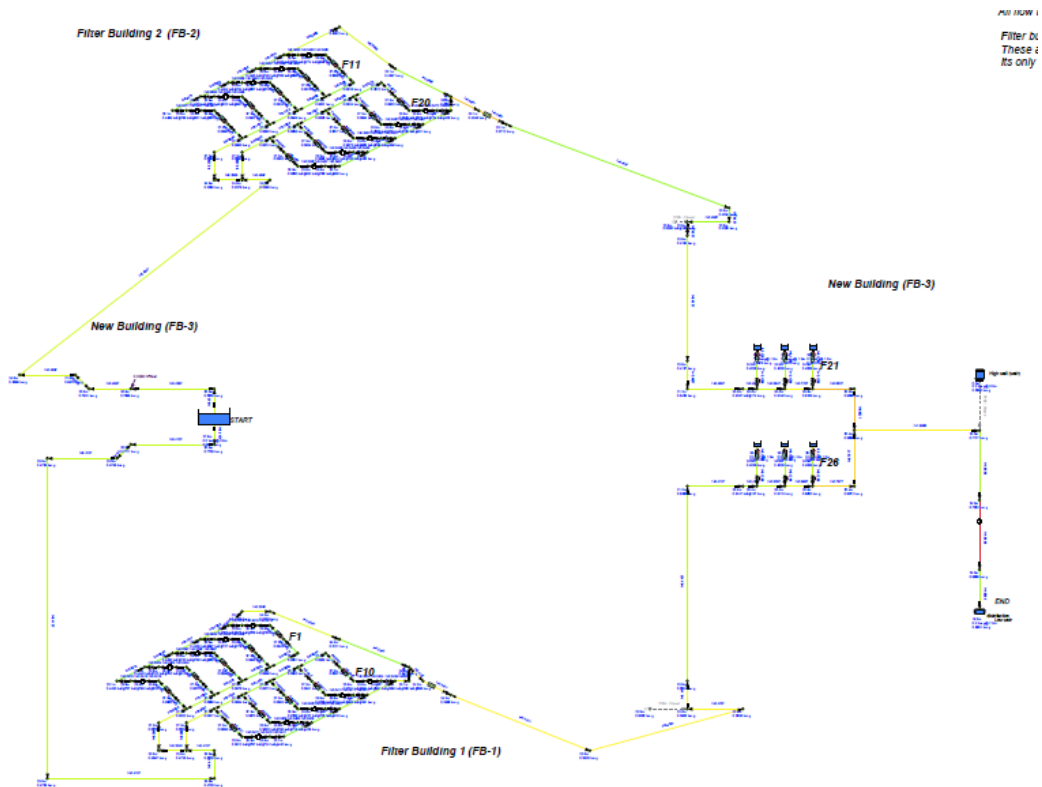


Figure 8-1: Model layout with flow velocity pattern.

During the investigation of the plausible measures to reduce the energy losses in the system the model was run with and without the components discussed above. The results are presented in table below.

Note: The system can give a maximum flow of 1651.5 l/s while in its current state with the filters in block 3 set at 129 l/s. Results for the investigation of the effect of some components to the system performance when they are removed from the system. This was done when the valves were 100% open

Table 8-1: Investigating the impact of the plausible measures.

| Components to be removed | Flow from FB1 (l/s) | Flow from FB2 (l/s) | Pressure before the disinfection basin | Total discharge (l/s) | Flow gain (l/s) |
|-----------------------------------|---------------------|---------------------|--|-----------------------|-----------------|
| Both Venturi meters | 457.7 | 539.4 | 0.6891 | 1771.1 | 120.0 |
| Valve before Venturi-meter in FB1 | 412 | 466 | 0.6886 | 1651.6 | 0.1 |
| Venturi and valve in FB1 | 459.5 | 539.2 | 0.6891 | 1772.7 | 121.2 |
| Venturi, valve and weir | 474.4 | 556.8 | 0.6893 | 1805.2 | 153.7 |

The 800mm bends and the 1200mm tee junction in filter building 3 can be bypassed by connecting block 1 and 2 directly to the reservoir and then install the Ultra-Violet light equipment after the reservoir. Investigation results when block 1 and 2 are connected directly to the reservoir with the Venturi-meters, valve before the Venturi in FB1, and the weir removed

Table 8-2: Direct connection of FB1 and 2 to the reservoir

| Action | Discharge FB1 (l/s) | Discharge FB2 (l/s) | Flow increment (l/s) |
|--------|---------------------|---------------------|----------------------|
| | | | |

| | | | |
|---|-------|-------|-------|
| Direct connection of FB 1 and 2 to the reservoir with Venturi, valve and weir removed | 852.5 | 860.6 | 835.6 |
|---|-------|-------|-------|

Another investigation was the pressure at the exit nodes of each of the blocks 1 and 2 if they were connected directly to the reservoir with respect to specified discharge demands without first going through block 3. These are shown in table 8-3 below.

Table 8-3: Investigation results of pressure at the exit point after weir in bar.g

| Demands (l/s) | With all components | | Without Venturi & valve | | No Venturi, valve & weir | |
|---------------|---------------------|-------------|-------------------------|-------------|--------------------------|-------------|
| | FB1 (bar.g) | FB2 (bar.g) | FB1 (bar.g) | FB2 (bar.g) | FB1 (bar.g) | FB2 (bar.g) |
| 400 | 0.3990 | 0.4690 | 0.4359 | 0.5049 | 0.3023 | 0.4425 |
| 500 | 0.3291 | 0.4129 | 0.3854 | 0.4677 | 0.2552 | 0.4060 |
| 600 | 0.2492 | 0.3488 | 0.3260 | 0.4234 | 0.1999 | 0.3624 |

8.2 Cost implications for all actions made

When any of the actions in table 8-1 and 8-2 was implemented, Vombverket will be in position of securing a given annual sum of money assuming it was running at full capacity. Note: kr – Swedish kronor.

Table 8-4: The cost benefits for each action made

| Components to be removed | Flow increment (l/s) | Flow (m ³ /s) | Amount per year (m ³ /year) | Cost of water (kr) |
|-----------------------------------|----------------------|--------------------------|--|--------------------|
| Venturi meter | 120.0 | 0.1206 | 3.8 million | 13.3 million |
| Valve before Venturi meter in FB1 | 0.1 | 0.0011 | 35,000 | 122500 |

| | | | | |
|---|-------|--------|--------------|--------------|
| Venturi and valve in FB1 | 121.2 | 0.1222 | 3.9 million | 13.7 million |
| Venturi, valve and weir | 153.7 | 0.1537 | 4.9 million | 17.2 million |
| Direct connection of FB 1 and 2 to the reservoir with Venturi, valve and weir removed | 835.6 | 0.8356 | 26.4 million | 92.4 million |

For any action taken, there will be a service cost. This will include the labor costs and the cost of elements to replace the removed component like a piece of pipe to replace the venturi-meter. The costs in table 8-4 are as per the amount charged per m³ of delivered water (3.50kr) without considering the other fixed fees (for Sydvatten)

If a pump is to be installed, then the best position was found to be after each filter block. That's to say after the weir. This give chance for the weirs to regain their functionality. But then there will be costs involved including but not limited to, service and maintenance costs, electricity costs and fitting costs. The pumps' job will be to overcome the high resistance in the system just after the weirs i.e. Against the 800mm bends, the 1200mm Tee junction and the constriction for the main flow meter. Therefore, the pumps need to be low-head pumps just enough for the job.

Electricity costs 1.0kr/KWh for Vombverket (kraftringen, 2016). Therefore, to get the total energy consumption in KWh, the equation below was used,

$$E(KWh) = Power (KW) \times Time (hr) \quad (8.1)$$

| | | |
|---|---|--|
| <p>Pump Data</p> <p>Name: Pump Catalog: General Manufacturer: Generic Type: End suction Size: 10x8-13 A100 Stages: 0</p> <p>Speed: 1470 Rpm Impeller Diam: 327.000 mm</p> <p>Min Speed: 750 Rpm Max Speed: 1475 Rpm Min Diam: 266.700 mm Max Diam: 336.550 mm</p> | <p>Fluid Data</p> <p>Fluid: Water Density: 998.000000 kg/m³ Viscosity: 1.0020 cP Temperature: 20.000 °C Vapor Pressure: 0.0240 bar.a Atm Pressure: 1.0132 bar.a</p> | <p>Operating Notes</p> <p>Pref. Op. Region: 70% - 130% of BEP Pref. Flow Range: 0.1150 - 0.2136 m³/sec</p> <p>Notes: This pump performance is generally similar to certain ranges from these pump manufactures: Ansi Pro AP96, Goulds 3196, Peerless 8196, Griswold 811, Summit 2196 & Durco Mark III Series ANSI pumps</p> |
| | <p>Design Curve</p> <p>Shutoff Head: 36.376 m.hd Fluid Shutoff dP: 3.5601 bar.g BEP: 84.7% @ 0.1643 m³/sec Power at BEP: 49.26 kW NPSHr at BEP: 4.325 m.hd Fluid Max Flow Power: 53.81 kW @ 0.2191 m³/sec</p> | <p>Data Point (BEP)</p> <p>Flow: 0.1643 m³/sec Head: 25.948 m.hd Fluid Efficiency: 84.71% Power: 49.26 kW NPSHr: 4.325 m.hd Fluid</p> |

Figure 8-2: Pump power consumption of 49.26KW (pipe flow expert database)

Assuming the pump runs for 8 hours a day then, using equation 8.1;

$$E \text{ (KWh)} = 49.26 \text{ KW} \times 8 \text{ hr} = 394.08 \text{ KWh per day.}$$

$$= 143839.2 \text{ KWh per year}$$

Therefore, at the price of 1.0 kr/KWh, 144,000 kr would be spend for each pump on electricity bills alone per year. There would be four (4) pumps hence 576,000 kr for four pumps every year. On top of this cost add the other costs mentioned before and the pump purchasing price.

DISCUSSION, RECOMMENDATIONS AND CONCLUSION

9.1 Discussion

The study focus was the hydraulic system between the mixing chamber and the disinfection tank. The system set to start at an elevation of +28.44m (water surface) with a water column of 0.64m. as water enters the mixer from aeration, it flows over the weirs into an open channel system that distributes it. 1/3 of the water flow to the FB1, another 1/3 to FB2 and the final 1/3 of the flow joins the filters 21 to 26.

Assumption 1.

The water level in the mixing chamber is approximately equal to the water level in the channels so a standard water level was assumed for the basin and the open channels distributing to the filters and blocks 1 and 2.

Also note that the water level can't go above +28.45m as a precaution to prevent overflow hence flooding with in building 3. (Persson. T, 2015).

The energy loss increases and the flow rate increases in the system. Water flows through a series of short length pipes and numerous fittings as discussed in the previous chapters.

There is rigorous turbulent flow at the 700mm vertical pipe taking water from the open channels to filter blocks 1 and 2. This is as a result of huge amounts of air sucked into the system. This air ends up into the pipeline forming pockets that create lots of resistance to water flow. The line to FB2 has a 200mm pipe that connects to it at right angle bringing 29 l/s of treated backwash water back into the system. This pipeline acts as an escape route for the air sucked in the 700mm pipeline. This reduces the resistance due to air locks in this line. This was the motivation for the adjustment of the filter resistance in block 2 during calibration.

Assumption 2.

The 29 l/s of clean backwash water is assumed to be continuously added to the system at any time.

The line to FB1 is not having any connection hence having a very high resistance due to air locks in the pipeline. This is visible through the continuous

air bubbles that are in filters 6 and 10. There is less air bubbling in FB2 filters. It was also observed that the water level in filter 6 and 10 is a bit lower at least by 1 decimeter compared to the rest of the filters. Hence water resistance in the line to FB1 is higher than that to FB2 following the survey made on May 8, 2015 at two different times when the water level was 1.0 -1.1m and 1.15-1.25 below the edge of the basins in FB2 and FB1 respectively at a flow of 400l/s (Persson. T, 2015)

Assumption 3.

For this study therefore, the modeler assumed the water level in all the 20 filters in FB1 and FB2 to be equal. The filters were also assumed to have the same characteristics and properties hence represented by the same curve loss before calibration.

After calibration, the properties of the filters in FB2 was adjusted making them different from those in FB1 but it remained that all filters in the same block had the same properties and characteristics.

The weirs at the end of both blocks 1 and 2 are completely submerged, this leads to a complete loss of all the kinetic energy (K.E) generated in the pipeline to potential energy (P.E). This changes the performance of the system and the model since this weir basin would be recognized as an infinite source by pipe flow expert model giving inaccurate results.

Assumption 4.

The modeler therefore assumed that this loss, due to conversion from K.E to P.E, is very negligible but present the weir as a node with exit and entrance losses.

The visualization of the hydraulic profile through the system with respect to elevations is shown below

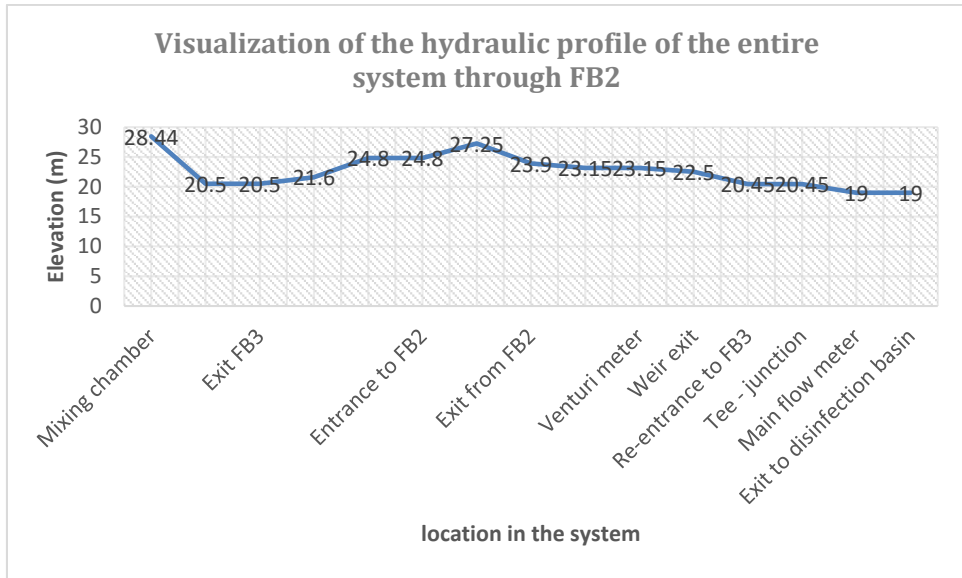


Figure 9-1: Hydraulic profile of the system through FB2

A visualization for pressure profile through the system considering the route through FB2

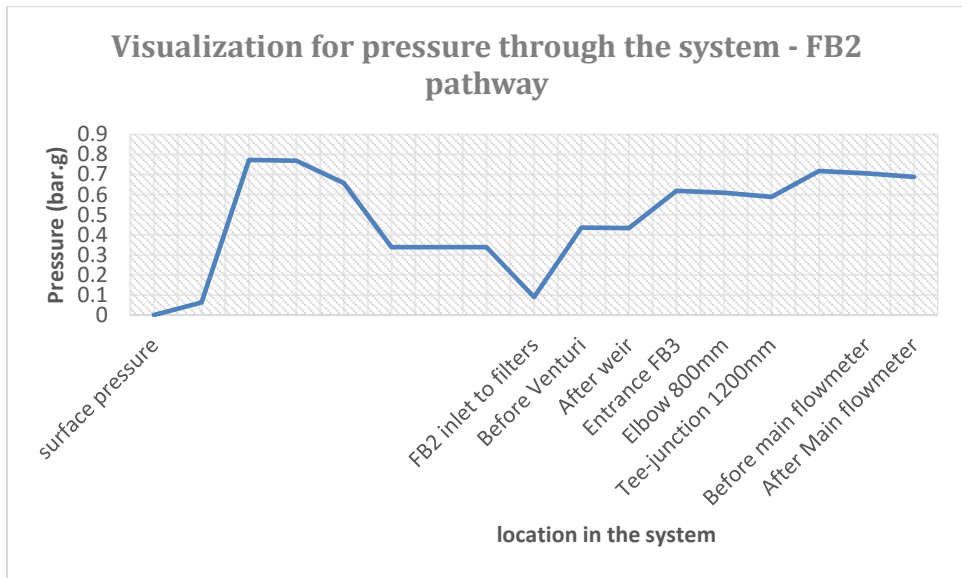


Figure 9-2: Pressure profile visualization - FB2 pathway

Why is the flowrate in FB2 greater than that in FB1?

1. The extra added volume from the cleaned backwash water of 29l/s
2. The low resistance due to air pockets and turbulence as discussed before and reduced head loss in the last section of FB2 compared to FB1.

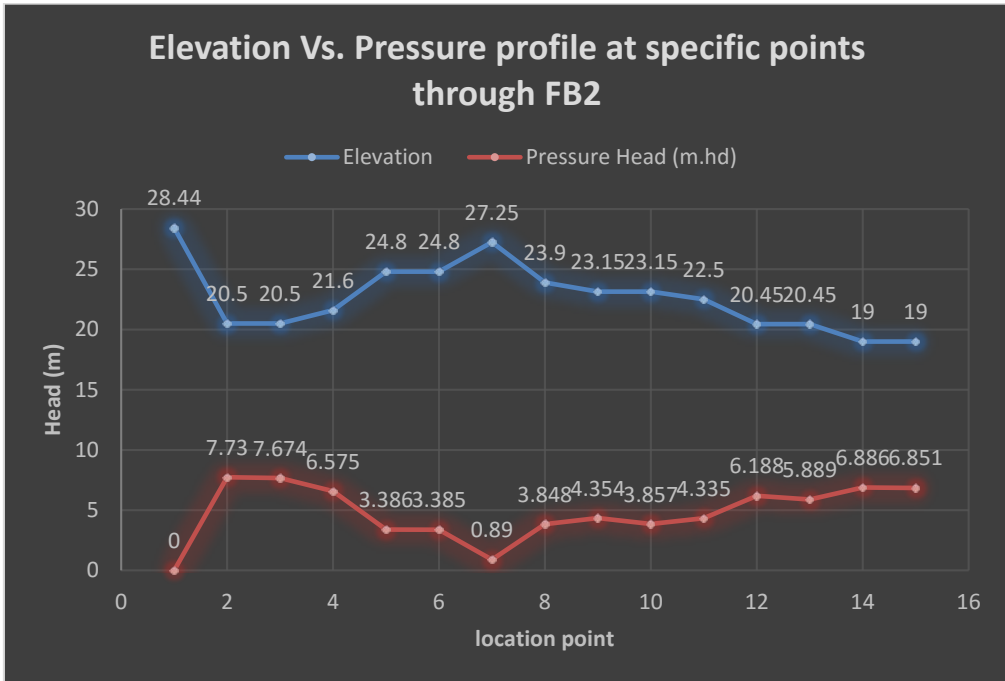


Figure 9-3: Elevation Vs. Pressure head profile through FB2

Before expansion in the 1990s, water took a very short flow path hence the exposure to pipe friction, local losses and turbulence was limited. After expansion the flow path increased, a lot of new fittings and pipe connections introduced together with hydraulic structures. The resistance to water flow increased and this is evident with the simulation of the system operation as of today vs. the system operation when FB1 and 2 are connected directly to the reservoir that is directly opposite the new building (FB3). The flow is seen to increase as shown in table 8-2 in the previous chapter.

Table 9-1: Present system design vs. direct connection to the reservoir.

| Performance | FB1 (l/s) | FB2 (l/s) |
|-------------|-----------|-----------|
|-------------|-----------|-----------|

| | | |
|--------------------------------|-------|-------|
| Now (100% valve opening) | 411.9 | 465.7 |
| Direct connection to reservoir | 852.5 | 860.6 |

Appendix (11-3), is the layout of the system when directly connected to the reservoir.

Tables 8-1 and 8-2 above show the investigation results of the plausible measures to increase the capacity of the system and reduce significantly the energy losses within the system. From the simulation results its observed that at full system capacity i.e. When all the valves are 100% open, the venturi-meter in FB1 offers the following pressure value as compared to other elements on the same link under similar conditions of 411.9 l/s flow rate with a velocity of 1.457m/s.

Table 9-2: Comparison of head losses between components on the same link under similar conditions

| Component | Head loss (m.hd) – FB1 (411.9l/s) | Head loss (m.hd) – FB2 (465.7l/s) |
|----------------------|-----------------------------------|-----------------------------------|
| Venturi-meter | 0.387 | 0.491 |
| Exit loss | 0.119 | 0.14 |
| Gate valve | 0.011 | 0.014 |
| Pipe friction losses | 0.007 | 0.006 |

It can be clearly observed that the venturi meter imposes a higher resistance to flow and its removal would create a great relief to the system boosting up the capacity of the system as viewed in tables 8-1 and 8-4.

Weir; having noted earlier that it leads to loss of the K.E to P.E, it also exposes the system to added losses like the exit and entrance losses that are also relatively significant for example. At a flow of 411.9 l/s in FB1, the entrance losses were recorded as 0.054m.hd. when these two losses are added up would give a whopping 0.173 m.hd which when compare to the overall drive in the system is very significant. Removal of the weir is highly significant.

The Gate valve in FB1 causes a comparatively low head loss of 0.011 m.hd compared to the other fittings being questioned but its removal is seemingly important since it is no longer in use. If the weir, Venturi-meter and the valve

in FB1 are removed, the model shows a very significant boost in both pressure and capacity (discharge) in the entire system and exhibited by tables 8-1 and 8-3.

The measure that gives the highest boost to the system is when FB1 and FB2 are directly connected to the reservoir. But this will require further modeling to check for the effect of the U.V light disinfection device to the system in terms of energy losses.

The effect of the U.V light disinfection device was not modelled in this study because the management at the plant decided to change the proposed location from the point near the disinfection basin to the point after the reservoir, a point far outside the study scope for this thesis.

9.2 Recommendations

The recommendation can be broken down into two; Category one and two as discussed in the sections below.

9.2.1 Category one

Having observed the behavior of the Vombverket hydraulic system by simulating different scenarios using pipe flow expert, better results were obtained when the venturi-meters in both FB1 and 2, gate valve in FB1 before the venturi and the weir basins in both blocks 1&2 were removed. A significant increase in both system pressure (driving force) and the discharge from the two highly affected blocks (1 &2) was recorded.

This action has the following additional merits if it were adopted at the plant:

1. Time saving: it would take a relatively short period of time to replace the components with pieces of pipe without creating huge inconveniences in demand. One block is closed and replacements made while the other is in operation and vice versa. It would take a limited time for both blocks and the entire system to be back in full operation with an improved capacity.
2. It's easy to be done: It's an easy process that doesn't require any special technics and expertise but only plumbing skills.

3. There are no extra constructions (civil works) required. The plant remains with the same layout as before but improved with better performance.

Demerits:

1. If it's assumed that the population of skåne would double in the near future with many more municipalities coming on board, demand is assumed to double. This means that the production would not be enough because the system offers an increment of 178.9 l/s.

9.2.2 Category two

If the system is sought to be built back to more than the as build performance, then bypassing as many of the plausible components causing the resistances to flow as possible is required. The water flow path must be made as short and smooth as possible. This involved simulation of the plant hydraulic system with all the components discussed in chapter 8, removed but this time and additional action is done. Filter blocks 1 and 2 are disconnected from the system and connected directly to the reservoir located just opposite the new filter block (FB3).

Since the chloramine dosing (disinfection basin) chamber would be bypassed, there would be need to install another disinfection mechanism and this time around it's the U.V light disinfection device. The device's possible and suitable location would be after the reservoir but before the pumping stations.

The action has the following additional merits;

1. Like discussed in the previous section about population increase and doubling of demand, this action will offer an increment of 835.6 l/s which is approximately a doubled discharge from each of the blocks 1 and 2. This action can suit the required demands even if the demands doubled.
2. There is room for improvement of the system layout and incorporation of new components into the system hence highly improving the efficiency and performance of the Vombverket water treatment plant hydraulic system.

3. The plant would get a more “*resilient design*” and be “*Built back better*”

Demerits

1. It is not advisable and not allowed to operate the Vombverket hydraulic system at these flowrates of 852.5 l/s and 860.6 l/s from block 1 and 2 respectively because the filtration function will be highly compromised (decreased). The filters in both blocks are designed for a combined allowable flowrate of between 500 -600 l/s from each block. Beyond this the quality of water is compromised.
2. The initial investment would be very high
3. The system becomes more complex and lots of studies must be undertaken and further simulation and modelling done to clearly understand the plausible performance of the new system layout.
4. Additional civil works will have to be done during the connection of the two blocks to the reservoir. This will involve breaking of structures for access, trenching, new access manholes, new shelter for the U.V device and control room.
5. New calculations and design procedures for the pumps and reservoir needed due to the enormous new discharge generated.

Depending on the possible allowable budgeting and acceptance by the management, stakeholders and politicians; one of the above recommendation can be chosen at a time.

9.3 Conclusion

It is true the expansion of the hydraulic system at Vombverket in the 1990's led to the deterioration of the plant performance in terms of capacity and pressure. A thorough investigation for the possible sources, locations and properties of the energy loss was done. The different cost effective measures after validation of model were explored and the optimum one identified. This was made possible by pipe flow expert model that indicated all parts of the system with a velocity color pattern clearly showing the areas with the highest velocities which is indicative of a high degree of energy losses.

The procedure of the sensitivity analysis helped to ease the calibration process of the model in a sense that, the most important parameters to which the model is highly sensitive were identified. A clear definition of which parameters/variables were dependent and independent was done making it possible to know which variables should be adjusted and the ones whose sensitivity is being sought.

Calibration helped to improve the performance and characteristics of the model especially the part in filter block 2 that was in disagreement with the measured/observed results. A perfect fit of the model results and measured results in terms of node pressure and discharge was obtained in all the sections of the system. Additional datasets were used to determine whether the model was suitable for the system in the validation stage which all produced a perfect match between the observed and model results.

Simulation of the different scenarios of the plausible and possible measures which would improve the system performance were carried out and their cost implications evaluated and determined on an individual and later combined basis.

The researcher made recommendations which he categorized as one and two leaving the final decision to the stakeholders to choose the most appropriate and suitable solution depending on the allowable budgeting and regional future anticipated plans.

For an optimized result, category one should be adapted but for a maximized result with flow control valves in place to ensure that the maximum flow range of 500-600l/s from block 1 and 2 is not exceeded for quality purposes, category

two would be appropriate. This is with reference to the costs involved to execute any of the two measures verses the returns, quality and demand.

REFERENCES

1. Andrew Sleigh and Ian Goodwill, (2009) "*CIVE2400- Fluid Mechanics: Fluid flow in pipes*" University of Leeds. Available at: <https://sipil2010.files.wordpress.com/2011/08/pipe-flow-5.pdf>. Accessed on: 4/4/2016
2. Crane Co, (1988) "*flow of fluids through valves, fittings and pipe*" Crane Engineering Department. Technical Paper No. 410. Available online at: <http://uolab.groups.et.byu.net/files/pipefitt/hints/1988Crane.pdf> Accessed on: 4/11/2016
3. Da Silva, M.G., de Oliveira de Aguiar Netto, A., de Jesus Neves, R.J., do Vasco, A.N., Almeida, C. and Faccioli, G.G. (2015) "*Sensitivity Analysis and Calibration of Hydrological Modeling of the Watershed Northeast Brazil*". Journal of Environmental Protection, 6, 837-850. <http://dx.doi.org/10.4236/jep.2015.68076>
4. Henryk Kudela, (2001) "*Hydraulic losses in pipes*" Wroclaw University of Science, Poland. Available at: http://fluid.itcmp.pwr.wroc.pl/~znmp/dydaktyka/fundam_FM/Lecture11_12.pdf. Retrieved on: 13/2/2016
5. Kraftringen, (2016) "*Our current electricity prices*" - Lund city. Available at: <http://kraftringen.se/Privat/El/Vara-elpriser/>. Accessed on: 5/6/2016
6. Larock, B.E., Jeppson, R.W., and Watters, G.Z. (2000). "*Hydraulics of Pipeline Systems*", CRC Press, ISBN: 0-8493-1806-8.
7. Paul Boulos and Tom Altman, (1991) "*A graph-theoretic approach to explicit nonlinear pipe network optimization*" Appl. Math. Modelling. Vol. 15. Published by: Butterworth-Heinemann. Available at: <http://www.sciencedirect.com/science/article/pii/0307904X9190035N> retrieved on: 1/4/2016
8. Persson, T., Bergengren, A., and Britt-Marie, P. (2015). "*Snabbfilterutredning på Vombverket*", Sydsvatten rapportserie 2015-001. Diarienummer: SV/2015/014-1
9. Pipe Flow Expert, (2016) "*User Guide*" Available in: Pipe Flow Expert v7.30 Model Software "Documentation"
10. Ratnayaka, D.D., Brandt, M.J., and Johnson, M. (2009). "*Water Supply*" (Sixth Edition) Elsevier, 744 Pages, ISBN: 978-0-7506-6843-9.

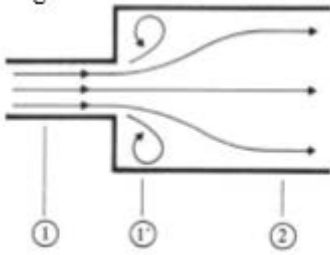
11. VASYD, (2016) "Avgifter för dricks – och avloppsvatten för villor i malmö stad" www.vasyd.se/va-taxa org nr: 222000-2378
12. Vennard, J.K. and Street, R.L. (1982). "Elementary Fluid Mechanics" (Sixth Edition), John Wiley, ISBN 047104427X.
13. Yunus, A. Cengel, John, M. Cimbala (2006a) "Fluid Mechanics: Fundamentals and Applications" Chapter 8: Flow in pipes. ISBN: 0-07-247236-7. Published by: McGraw-Hill. Available at: https://www.uio.no/studier/emner/matnat/math/MEK4450/h11/undervisningsmateriale/modul-5/Pipeflow_intro.pdf. Retrieved on: 1/2/2016
14. Yunus, A. Cengel, John, M. Cimbala (2006b) "Fluid Mechanics: Fundamentals and Applications" Chapter 5. ISBN: 0-07-247236-7. Published by: McGraw-Hill. Available at: https://www.uio.no/studier/emner/matnat/math/MEK4450/h11/undervisningsmateriale/modul-5/Pipeflow_intro.pdf. Retrieved on: 1/2/2016

APPENDICES

Appendix A

A.1 Analytical derivation of the K-Factor expression

A.1.1 Sudden Expansion and Exit losses into a tank



Therefore applying the momentum Equation (Eqn. 2-7)

$$P_1A_1 - P_2A_2 = \rho Q(u_2 - u_1)$$

And also from the continuity equation (Eqn. 2-3) and replace for Q in Eqn. 2-7,

$$P_1A_1 - P_2A_2 = \rho u_2A_2(u_2 - u_1)$$

Rearranging the variables and dividing through by ρg on both sides will give,

$$\frac{P_1 - P_2}{\rho g} = \frac{u_2}{g} (u_2 - u_1)$$

(11-1)

So, taking the Bernouli's Eqn between point 1 and 2 on the figure above

$$\frac{P_1 - P_2}{\rho g} - \frac{(u_1^2 - u_2^2)}{2g} = h_l$$

(11-2)

Substitute (7-1) into (7-2)

$$\frac{u_2}{g} (u_2 - u_1) - \frac{(u_1^2 - u_2^2)}{2g} = h_l = \frac{1}{2g} (u_1 - u_2)^2$$

Substitution from the continuity equation for $u_2 = \frac{u_1A_1}{A_2}$

$$h_l = \frac{1}{2g} (u_1 - u_2)^2 = \frac{1}{2g} \left(u_1 - \frac{u_1A_1}{A_2} \right)^2 = \frac{u_1^2}{2g} \left(1 - \frac{A_1}{A_2} \right)^2$$

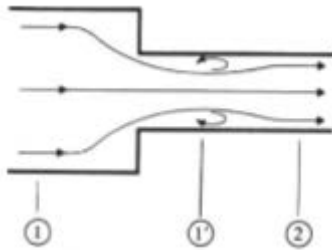
(11-3)

Therefore from Equation. 2-22, the K-factor is given as;

$$K = \left(1 - \frac{A_1}{A_2}\right)^2 \quad (11-4)$$

For A_1 and A_2 are the Areas for section 1 and 2 of the pipe respectively. When $A_1 \ll A_2$ I.e $\frac{A_1}{A_2} = 0$ then, that means $K=1$ for exit losses into a tank.

A.1.2 Sudden contraction and entrance losses



Here flow contracts from section 1 to 1' forming a vena contracta. From experiments, it's assumed that the vena contracta area at 1' is approximately 40% of the A_2 therefore, taking continuity at 1' and 2 $u_{1'} = \frac{u_2 A_2}{A_{1'}} = \frac{u_2 A_2}{0.6 A_2} = \frac{u_2}{0.6}$

Substitute this into equation (7-3)

$$h_l = \frac{(u_2/0.6)^2}{2g} \left(1 - \frac{0.6 A_2}{A_2}\right)^2 = 0.4 \frac{u_2^2}{2g}$$

Finally, the value of K for sudden contraction is approximately 0.4

Appendix B

B.1 Graphical representations of the experimental determination of the K-factor for pipe fittings

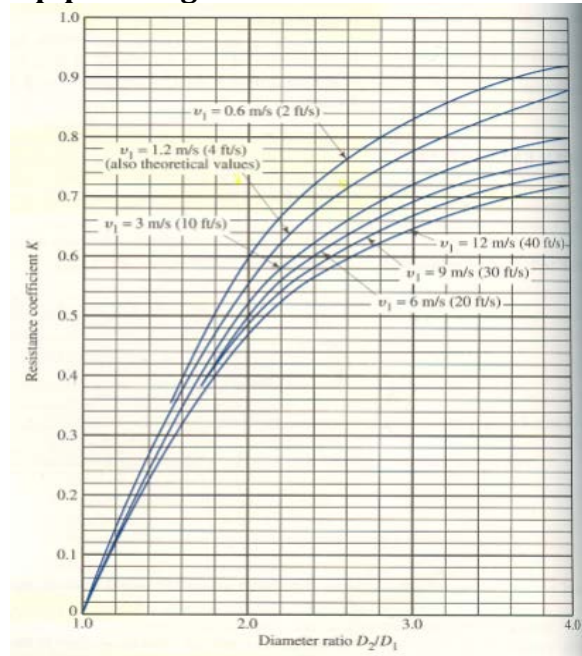


Figure 11-1: K-value for sudden enlargement

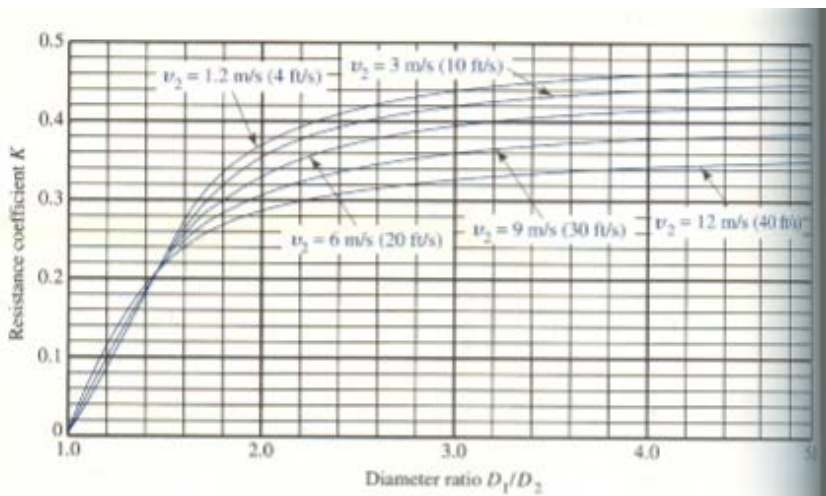


Figure 11-2: K-value for sudden contraction

Appendix C

C.1 Flow meter characteristics as obtained from manufacturer's catalogues

Table 11-1: Volumetric flowmeter characteristics

| Type | Typical pipe diameter (D) range (mm) | Typical velocity range (m/s) | Typical accuracy (% of full scale) | Typical repeatability (% of full scale) | Typical head loss coefficient (K) | Comment |
|--------------------|--------------------------------------|------------------------------|------------------------------------|---|--|--|
| Volumetric | | | | | | |
| Electro-magnetic | 25–2500 | 0.5–10 | 0.25 | 0.1 | 0 | |
| Ultrasonic | Up to 7000 | 0.05–4 | 1 | 0.5 | 0 | Sensitive to vibration and head alignment |
| Coriolis | 15–80 | 0.5–5 | 1 (of mass) | | 15 | May include density measurement with accuracy about 0.4% |
| Vortex | 15–300 | 0.4–10 | 1 | 0.2 | 2 | Not suitable for pulsating flow |
| Turbine | 15–400 | 0.6–10 | 0.5 | 0.1 | 0.8 | |
| Rotating vane | 15–150 | 0.02–6 | 1 | | 5.5 | |
| Rotating piston | 15–20 | 0.03–4.4 | 2 | | 4 | |
| Paddle wheel | 15–1000 | 0.3–6 | 1 | 0.5 | 5.5 | |
| | | | | | Head loss as % of pressure difference | |
| Inferential | | | | | | |
| Venturi tube | 50–1200 | | 1.25 | | 10–20 | Length = 5D |
| Dall tube | 150–2000 | | 1.25 | | 30 | Length = 1.75D |
| V cone venturi | 15–3000 | | 0.5 | 0.1 | Up to 75 | |
| Orifice plate | 25–200 | | 3 | 1 | Up to 90 | |

Appendix D

D.1 System layout for direct connection to the reservoir

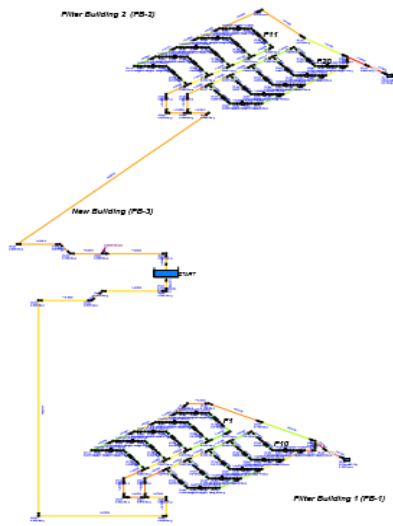


Figure 11-3: Model layout for direct connection to reservoir



Above is the interior view of FB2. This is similar to FB1 layout

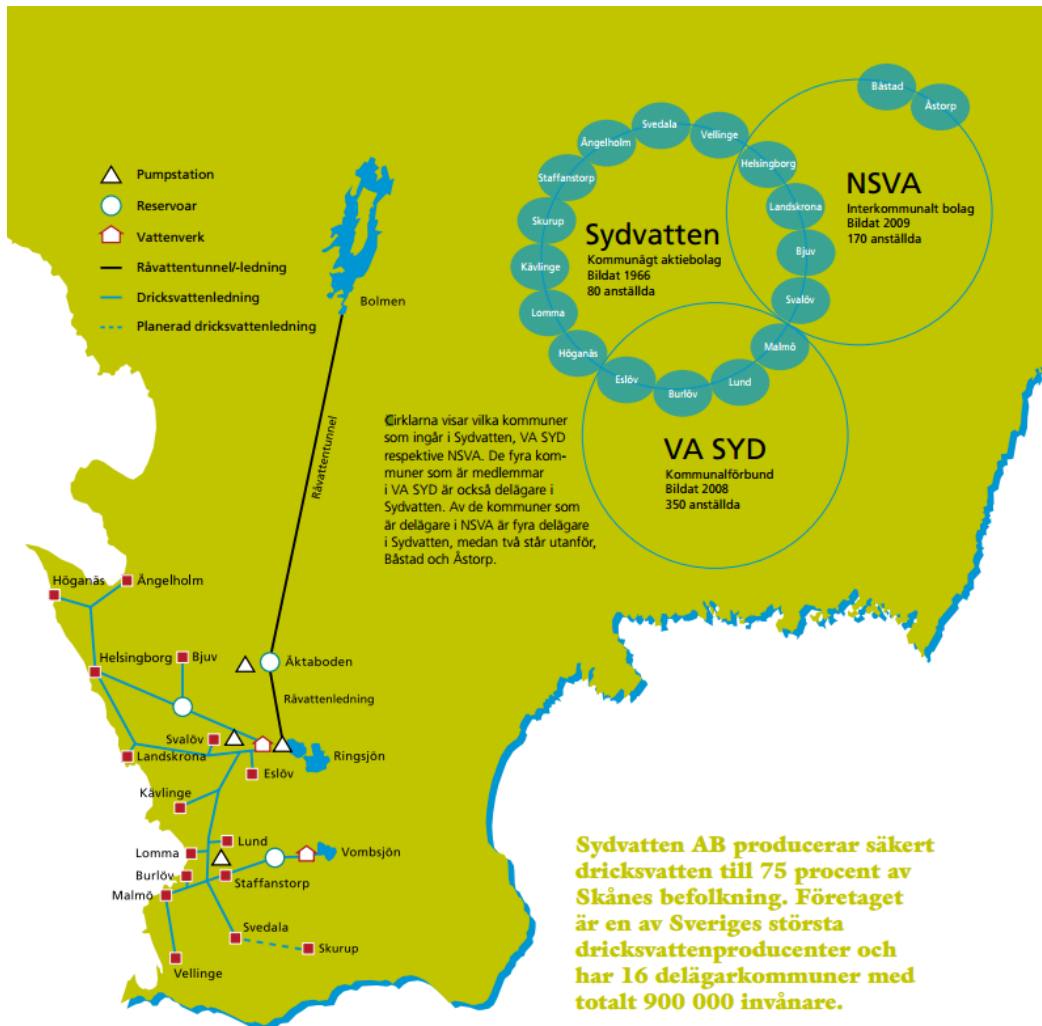


Figure 11-4: Map showing the location and distribution network of Vombverket (Sydsvatten,2016)

The interior of filter building 2



Below is the pictorial view of the mixing chamber where the study begins

